Vibrational and Rovibrational Spectroscopy Applied to Astrochemistry

Ryan C. Fortenberry*,† and Timothy J. Lee*,‡

†*Department of Chemistry & Biochemistry, University of Mississippi, University, MS 38677-1848*

‡*MS245-3, Planetary Systems Branch, Space Science and Astrobiology Division, NASA Ames Research Center, Moffett Field, CA 94035, USA*

E-mail: r410@olemiss.edu; timothy.j.lee@nasa.gov

Abstract

The detection of molecules in astrophysical environments almost always requires remote sensing. While radioastronomical observation and associated rotational spectroscopy are powerful astronomical tools, infrared spectral analysis provides a unique means of examining the observable universe, especially for molecules where permanent dipole moments are small or even non-existent. The molecular vibrations of small molecules are now able to be modeled via quantum chemistry and electronic structure theory conjoined to vibrational analysis to within spectroscopic accuracy in many cases. This chapter will showcase this success and build upon it to show how such advances are now being leveraged to describe molecular vibrations for molecules containing dozens of atoms, electronically excited states, "hot bands," exoplanetary atmospheric opacity data, and even emission of polycyclic aromatic hydrocarbons. All of these are required to prune the interstellar spectral garden of its "weeds" in search of "flowers" that will provide the necessary fingerprints for astronomers to be able to probe the heavens for its past, present, and future secrets.

Introduction

Quantum chemistry and electronic structure theory have played a crucial role in the detection of molecules in space largely since molecules have been detected in space. In the early- and mid-1970s radioastronomical observations were increasing the census of extraterrestrial molecules nearly from zero. Observation of the protonated nitrogen cation (N_2H^+) was among the first detection studies and also among the first that utilized the self-consistent field (SCF) Hartree-Fock (HF) approach to compute an equilibrium geometry and provide corresponding rotational constants for comparison to astronomically-derived spectral constants.[1,2] Similarly, detections of C_2H, C_4H, and C_3N also employed a similar approach utilizing quantum chemical *ab initio* theoretical data for corroborating evidence of detection.[3–5] During this era, the famed "X-ogen" lines were reported,[6] but these lines were conclusively linked

to HCO^+ by Herbst and Klemperer[7] once more through the use of corroborating rotational constants derived from quantum chemically computed equilibrium molecular geometries.

In the decades since, quantum chemistry has spread its application in astrochemistry to more than just providing optimized geometries and the associated, complementary rotational constants, although this is still a vital service from quantum chemistry. With the growth in telescopic power and technology, notably for air- and space-based observatories, the infrared region of the electromagnetic spectrum is one of the, if not the, most important wavelength ranges for modern observations. IR photons can penetrate dust and also provide emissions from optically-thick regions where other wavelengths become opaque or convoluted. The ongoing usage of the *Stratospheric Observatory for Infrared Astronomy* (SOFIA) and the upgraded CRyogenic high-resolution InfraRed Echelle Spectrograph (CRIRES+) instrument at the European Southern Observatory (ESO) as well as the soon-to-launch *James Webb Space Telescope* will usher in a new era of unprecedented data for the near-, mid-, and far-IR regions. Hence, only the throughput and bottom-up approach of quantum chemistry and electronic structure theory can hope to provide the necessary volume and labeling of reference data for such large amounts of information to be gleaned from these observatories.

Recent work has already shown direct application of quantum chemistry to observations from SOFIA. Rovibrational lines determined, in part, from high-level, modern electronic structure computations have led to the first mid-IR detection of HNC and $H^{13}CN$ toward the Orion Hot Core.[8] Additionally, quantum chemical studies have provided the full set of fundamental anharmonic vibrational frequencies for protonated cyclopropenylidene (c-$C_3H_3^+$)[9] leading to its IR detection in the laboratory[10] as well as providing the target frequency range for ongoing SOFIA and CRIRES+ searches for this postulated precursor to larger interstellar hydrocarbon chemistry. Additionally, the determination of dense molecular line lists of rotational and rovibrational states is also a vital service provided by quantum chemical computations where thousands of lines can be provided for a single molecule without any gaps in the data. These are often empirically-refined for a few known lines providing

exceptional accuracies for the vast majority of unknown lines.[11–15] These such studies help to eliminate the so-called spectral "weeds" by pruning the unknown transitions of known molecules allowing for the potential observation of unknown transitions of unknown molecules (the "flowers"). Hence, the role of quantum chemistry in astrochemistry continues to grow especially with regards to molecular vibrations and their associated physics.

This present work will highlight the role of quantum chemistry in the determination of vibrational and rovibrational properties and spectral data for numerous applications to astrochemistry. While this review is intended to be broad, the applications of electronic structure theory and quantum chemistry to astrochemistry are even broader and seemingly endless. The single molecule nature of traditional quantum chemistry and the flexibility of study for terrestrially-unstable molecules makes it a natural fit for astrochemistry. Consequently, the applications of quantum chemistry, even computations of molecular vibrations, would stretch beyond any single review. Herein, we will focus on the emerging work where molecular vibrations utilizing electronic structure computations are vital including the aforementioned molecular line lists as well as the observation and constraining of polycyclic aromatic hydrocarbons (PAHs), small molecules of astrobiological significance, and even more exotic behaviors including molecular vibrations of electronically excited states. These areas highlight the ways in which the intramolecular motions of atoms within molecules hold vital significance for pushing the boundaries of knowledge for astrophysical implications. In so many ways, molecular vibrations are the fingerprints of astrophysics, and quantum chemistry provides the needed reference data for comparison.

Computational Aspects

Theoretical Framework

Most quantum chemical computations addressing molecular vibrations in some way rely upon the harmonic approximation. Such is sensible when molecular vibrations are the smallest,

meaningful contributor to the total energy, as is the case for computing reaction energies. However, when the molecular vibrations are the focus, more accurate representations are required. The venerable quartic force field (QFF), or fourth-order Taylor series approximation to the internuclear Hamiltonian's potential, has largely become the most-often utilized method for producing the anharmonic potential. Mathematically, the QFF is represented as:

$$V = \frac{1}{2}\sum_{ij} F_{ij}\Delta_i\Delta_j + \frac{1}{6}\sum_{ijk} F_{ikj}\Delta_i\Delta_j\Delta_k + \frac{1}{24}\sum_{ijkl} F_{ijkl}\Delta_i\Delta_j\Delta_k\Delta_l, \quad (1)$$

where the $F_{ij\ldots}$ terms are the force constants while the $\Delta_i\Delta_j\ldots$ terms are the displaced distances for coordinates i, j, etc. from a given reference geometry,[16,17] typically on the order of 0.005 Å and 0.005 radians. The reader should note that the reference point and the first derivative needed for a more complete Taylor series expansion appear to be omitted from Equation 1. In truth, the reference point is set to zero by construction, and the first derivative should be zero by definition if the reference geometry is, in fact, a minimum.

The coordinates (i terms in Equation 1) can take on many forms from Cartesians to Morse-cosine,[18] but most QFF computations discussed herein utilize symmetry-internal coordinates where applicable or the simple-internal coordinates if necessary. The symmetry-internals are made up of simple-internals so the two often work hand-in-hand. The INTDER program[19] developed by Wesley Allen and coworkers at the University of Georgia has proven to be a valuable tool in the construction and translation of coordinates especially between simple-internals, symmetry-internals, and Cartesians.

Regardless, such a representation as Equation 1 has been in use in quantum chemical electronic structure theory for many decades, and the evolution of such an approach for astrochemistry has been recently reviewed by numerous groups.[20–23] In truth, this is the lowest level anharmonic potential that can be constructed for consistently physically-meaningful representation of molecular vibrations. However, for most molecules, even those with seemingly bizarre electronic structure (bizarre in the terrestrial laboratory sense), the QFF is sufficient to describe the intramolecular atomic motions' potential energy.

However, the QFF is not the total computation. Once the potential has been constructed, it must be conjoined to the kinetic and kinetic-potential interaction portions of a larger vibrational model. The Watson Hamiltonian is the usual vehicle for such with rovibrational perturbation theory likely among the most straightforward means of using the QFF:

$$H = \frac{1}{2}\sum_{\alpha\beta}(J_\alpha - \pi_\alpha)\mu_{\alpha\beta}(J_\beta - \pi_\beta) - \frac{1}{2}\sum_k \frac{\partial^2}{\partial Q_k^2} - \frac{1}{8}\sum_\alpha \mu_{\alpha\alpha} + V(\mathbf{Q}). \quad (2)$$

In the above Equation 2, J_α represents the total angular momentum of a given cardinal direction ($x, y,$ or z) denoted by α or β. The π_α term is the total vibrational angular momentum of the same direction; $\mu_{\alpha\beta}$ is the inverse of the moment of inertia tensor for the given geometric coordinates; Q_k is a single normal coordinate; $\mathbf{Q}$ is the set of all normal coordinates; and $V(\mathbf{Q})$ is the potential portion, the QFF in this case.[9,24]

Like the QFF being the lowest-level anharmonic potential, even just second-order vibrational perturbation theory (VPT2) is enough to generate representations of molecular vibrations that are directly applicable to astrochemical problems. This has been extensively utilized through various VPT2 computer programs including the SPECTRO program[25] developed by Jeff Gaw, Nick Handy, and co-workers at Cambridge University with additions coming from the NASA Ames group. In short, VPT2 utilizes the harmonic approximation as the unperturbed portion of the computation. The cubic and quartic terms (third- and fourth-derivatives) in the potential represent the perturbation. Specifically, the Hamiltonian is split into the $\hat{H}_0$ (harmonic oscillator or quadratic terms from Equation 1) zeroth-order Hamiltonian as well as the two perturbation pieces: the $\hat{H}_1$ operator leading to the first-order correction to the energy comprised of cubic terms from the QFF and the $\hat{H}_2$ operator leading to the second-order correction to the energy comprised of the quartic terms from the QFF.[24,26,27] Both the first-order and second-order corrections to the energy come from the first-order wave function as is standard in Rayleigh-Schrödinger perturbation theory.[28] As a

result, the energy of a state can written as:

$$E_i = \langle\Psi^{(i)}|\hat{H}_0|\Psi^{(i)}\rangle + \sum_{n\neq i} \frac{|\langle\Psi^{(i)}|\hat{H}_1|\Psi^{(n)}\rangle|^2}{\langle\Psi^{(i)}|\hat{H}_0|\Psi^{(i)}\rangle - \langle\Psi^{(n)}|\hat{H}_0|\Psi^{(n)}\rangle} + \langle\Psi^{(i)}|\hat{H}_2|\Psi^{(i)}\rangle, \tag{3}$$

or, equivalently,

$$E_i = \epsilon_i + \sum_{n\neq i} \frac{|\langle\Psi^{(i)}|\hat{H}_1|\Psi^{(n)}\rangle|^2}{\epsilon_i - \epsilon_n} + \langle\Psi^{(i)}|\hat{H}_2|\Psi^{(i)}\rangle. \tag{4}$$

As with most Rayleigh-Schrödinger perturbation theory extensions such as the electronic structure MP2 theory,[29] VPT2 constructs a portion of the resulting perturbation energy to be solved in terms of the normalized square, or inner-product space, of the integral divided by the difference between the unperturbed (harmonic oscillator in this case) eigenvalues of two separate states i and n.[28] The $\hat{H}_2$ term is constructed in much the same way as the cubic, inner-product sum, but only the given $\langle\Psi^{(i)}|\hat{H}_2|\Psi^{(i)}\rangle$ piece survives by rules of matrix elements producing a simplified form of the anharmonic vibrational state energy in Equation 4.[27] There are other forms of this energy (with one given later in Equation 10 for asymmetric-top molecules), but the above is a more generic form of the VPT2 energy/frequency formulation.

Differently, vibrational configuration interaction (VCI) theory often utilized within the MULTIMODE program[30,31] developed by Stuart Carter and Joel Bowman along with their students and collaborators is another means of utilizing the QFF for computing molecular vibrational frequencies as well as other variational approaches. VCI has much more stringent requirements on the potential than VPT2 largely because variational methods access larger portions of the PES and, thus, require that it be positive definite or, in other words, not have any holes and not turn over at large coordinate values, largely since an actual wave function is created. These types of computations often require a global or semi-global potential energy surface (PES). However, if proper limiting behavior can be built into the QFF, even the smaller PES contained within a QFF can allow for QFFs to be utilized within VCI or other variational approaches.[18,32,33] Both VPT2 and VCI usage of QFFs have benefits and

drawbacks, and if the potential cannot be accurately represented, neither will perform well. Hence, the electronic structure computations of the displaced molecular geometries in any PES/QFF have really driven how meaningful quantum chemical computations of molecular vibrations are for application to astrochemistry.

QFFs in Practice

Agnostic to the level of theory, QFFs are implemented beginning with a tightly converged, optimized, minimum geometry. This is essential since the relative energies for the Δ_i step sizes (from Equation 1) can often be on the order of sub-milliHartrees even if the total electronic energy computed can be hundreds or thousands of Hartrees. The tight geometry convergence (10^{-6} Å or rad.) also requires that the computed correlation energies also be tightly converged (10^{-14} Hartrees) which also requires that the reference energy be tightly converged (10^{-16} Hartrees) which requires that the integrals must be tightly converged (10^{-20} Hartrees or probability for S integrals).[9]

From this optimized, reference geometry, a set of coordinates must be constructed in order to define the QFF properly. These coordinates are the i, j, k, l indices given in Equation 1. The coordinates can take on multiple forms,[18] but the most successful are typically the symmetry-internal coordinates. These are simply the symmetry-conserving coordinates made up of linear combinations of the simple bond stretches, angle bends, and torsional bends. Just like and closely related to the number of internal degrees of freedom, the number of coordinates for non-linear molecules is $3N - 6$, where N is the number of atoms in the molecule being examined. Typically and from practice, the heurestic for non-cyclic molecules is that if there N atoms, the symmetry-internal coordinate system will require $N-1$ stretches, $N-2$ bends, and $N-3$ torsions or out-of-plane bends. A simple coordinate set example is for triatomic ($N = 3$) water: the symmetric and antisymmetric bond stretches (2) as well as the bend therein (1) with no torsions. Such coordinates are akin to normal coordinates but are not mass-weighted allowing them to be utilized for different isotopic

substitutions without having to recompute the QFF.

Displacements of these coordinates define the Δ_n terms in Equation 1. Due to the vanishing integral rule, only those coordinates or products of coordinates that transform as the totally symmetric irreducible representation of the molecular point group are non-zero. For the water example, the quadratic or harmonic terms that survive are the second derivatives of each symmetry coordinate and the combined first derivatives of the bend and symmetric stretch. Hence, symmetry-internal coordinates reduce the total number of geometry points required for the QFF. The number of points grows geometrically with the number of atoms (N), and higher symmetry can alleviate such growth to some degree.

Once the coordinates are defined and the displaced geometries (often referred to simply as points) are constructed, the single-point electronic structure energies are computed at the desired level of theory. These are then gathered and turned into relative energies in order to reduce the numerical noise[34] for a least-squares fitting. The function fit is defined from the displacements of the coordinates and the resulting energies. The output of the fitting is the $F_{ij\ldots}$ in Equation 1. The function is then refit with the new stationary point (minimum in this case) included so that the gradients are truly zeroed and the remaining force constants are as precise as possible. These force constants can then be transformed as desired, and our experience is that construction of Cartesian coordinate force constants from simple-internal coordinate force constants allows for the most flexibility in the actual VPT2 comptuations. At this point, the VPT2 procedure then produces the anharmonic frequencies and spectroscopic constants for the molecule being examined. While QFFs are independent of the energy-type defining them, the choice of electronic structure method often is the principle dictation in the accuracy of the QFF conjoined to VPT2.

Predicting Vibrational & Rovibrational Spectra and Rovibrational Spectroscopic Constants to Identify Molecules in Astronomical Observations

The growth in accuracy of electronic structure methods, especially during the 1990s and 2000s, greatly enhanced the applicability of QFF-based anharmonic frequency computations to molecular vibrations with an eye towards astrochemistry. The "gold standard"[35] of coupled cluster theory at the singles, doubles, and perturbative triples level [CCSD(T)][36] especially with correlation consistent basis sets[37,38] has revolutionized *ab initio* quantum chemistry across nearly all fields ushering in notable accuracy for acceptable computational cost. However, the difference in chemical accuracy (typically thought of as 1 kcal/mol) and spectroscopic accuracy (typically 1 cm^{-1}) is orders of magnitude and many more significant digits. Higher convergence criteria are therefore required of both optimized, reference geometries as well as the energies themselves in QFFs that are tightly fit via a least squares procedure to construct the force constants. While CCSD(T)/cc-pVQZ was able to produce spectroscopic accuracy on a few occasions,[32,39,40] QFFs employing this and similar levels of theory were still in error compared to experiment by a variable amount on the order of tens of cm^{-1}.

Further enhancements to the actual energies used to produce the QFF have been able to reduce this error in vibrational spectroscopy to single wavenumbers routinely.[41] This consistency began with the use of a composite approach based on CCSD(T). Taking the CCSD(T) energy out to the complete basis set (CBS) limit and including perturbative effects for core electron correlation, relativity, and even higher-order electron correlation emerged in the mid-to-late 2000s.[42,43] Over the past decade, such an approach has consistently been employed to produce experimentally comparable results for vibrational, rotational, and rovibrational spectroscopic data playing part in the aforementioned laboratory detection of c-$C_3H_3^+$[9,10] as well as the detection of HSS (or S_2H) toward the Horsehead nebula among other suc-

cesses.[44,45]

Small Molecules in Their Ground Electronic States

CCSD(T)-Based Methods

While water is often the physical chemists' favorite molecule for testing various chemical models, astrochemically, employing H_2O as a test subject actually makes physical sense. After the uber-abundant diatomics in H_2 and CO, the most common molecule in various astrochemical environments is water.[46] Water was first identified in an astronomical observation in 1969 towards Sagittarius B2 (the nebula surrounding the center of the Milky Way Galaxy) as well as the Orion nebula via radioastronomical observation.[47] Water is also present in every body observed within our own Solar System and is the pervasive molecule in both gas- and condensed-phase astrochemistry. In 2008, it along with HO_2^+, were the first molecules to be examined with high-level composite energy QFF VPT2 computations.[42]

Water and HO_2^+ both show that the most accurate fundamental anharmonic vibrational frequencies of the methods explored include an initial CBS extrapolation involving the aug-cc-pVTZ/QZ/5Z basis sets using a three-point formula:[48]

$$E(l) = A + B\left(l + \frac{1}{2}\right)^{-4} + C\left(l + \frac{1}{2}\right)^{-6}. \tag{5}$$

While two-point extrapolations with the aug-cc-pVQZ/5Z basis sets behave in a similar fashion, the computational cost of the triple-ζ level is so small in comparison that its utilization is an addition that provides more certainty to the result with little cost. A two-point extrapolation with only the triple- and quadruple-ζ bases, however, is not as accurate. Inclusion of Douglas-Kroll scalar relativity[49] as a difference between the CCSD(T)/cc-pVTZ-DK energies with and without relativity included is added to the CBS energy. This provides a ~ 3 cm^{-1} gain in accuracy for all three modes. Finally, explicit and additive inclusion of core electron correlation is shown to have a non-negligible contribution to the final anharmonic

fundamental vibrational frequencies, as well.

The higher-order electron correlation is computed in this first approach via the averaged coupled-pair functional (ACPF) modification to multireference configuration interaction theory.[50] The difference in this energy at the cc-pVTZ level from the CCSD(T)/cc-pVTZ is also then added to the CBS+rel. energy for the QFF points giving a further shift of ~ 5 cm^{-1} and producing better agreement with experiment. The ACPF/cc-pVQZ computations are much more costly than the triple-ζ and most often have a less than 1 cm^{-1} shift in the fundamental frequencies. The so-called CBS+rel.+ACPF/TZ QFF coupled to VPT2 is within 4 cm^{-1} of experimental for all three fundamentals of water. While the same QFF with VCI is similarly accurate, both VPT2 and VCI produce stretching frequencies nearly indistinguishable from one another but differ by 4 cm^{-1} for the bend. Additionally, step sizes of 0.005 Å and 0.005 radians (the Δ_i values in Equation 1) are shown to be optimal in balancing energy shifts with known problems in minimizing higher-order numerical contamination of the force constants. HO_2^+ performs similarly giving indication that such an approach for computing anharmonic vibrational frequencies is a viable means for computing these values.[42]

This approach was verified shortly thereafter on a pair of anions: NH_2^- and CCH^-.[43] The C_2H radical was one of the first molecules observed in astrophysical media,[3] and anion forms of its longer family members (C_4H^-, C_6H^-, and C_8H^-) have also been observed.[51–55] NH_2 has also been observed towards Sgr B2[56] even though the anion form has been famously not detected in the same source despite ongoing searches.[57] In either case, the CBS+core+rel.+ACPF/TZ QFF behaves similarly compared to experiment for these two molecules of potential astrophysical significance further verifying the method. The major addition in this study is the inclusion of a core electron correlation composite term through the use of the Martin-Taylor core correlating basis set which actually pushes the CBS+core QFF frequencies away from experiment. This is brought back into agreement with experiment by including the relativity and ACPF terms.[43] Inclusion of the core correlation explicitly in the terms used for CBS extrapolations or as a composite energy term does not affect the overall

results by more than a single cm^{-1} or so, but it slows down the computation of the CBS terms by significantly more than the cost of the two composite energies. The implication is that the composite approach is the more effective execution for this piece of the QFF.

The method, however, was modified, again, a few years later in examination of c-/l-$C_3H_3^+$,[9] again of note for larger PAH synthesis.[58] Herein, the reference geometry is shown to require only CCSD(T)/aug-cc-pV5Z corrected compositely for core electron correlation for some geometrical parameter R:

$$R = R_{5Z} + (R_{MT(core)} - R_{MT(valence)}). \tag{6}$$

Addition of the other terms does not affect the reference geometry enough to warrant their inclusion. The Martin-Taylor (MT) core electron correlating basis set[59] is used at this point. From this geometry, the CBS+rel.+core+ACPF QFF is coupled to both VPT2 and VCI agreeing well with each other (within 10 cm^{-1}) and with the available experiment. Again, this work has informed experimental analysis of the ν_4 stretch of the cyclic isomer which was found to be 0.6 cm^{-1} less than the computed value at 3131.7 cm^{-1}.[10]

Such accuracies greatly inform the computation of the molecular vibrations for the *trans*-HOCO radical.[60] HOCO is believed to be a necessary intermediate in the synthesis of CO_2 in the Earth and Martian atmospheres and likely informs the carbon budget of similar gaseous regions.[61–63] At this point, the nomenclature for the QFF procedure is streamlined from CBS+rel.+core+ACPF to CcCRE with the "C", "R", "cC", and "E" terms coming from their respective counterparts in the form:

$$E(\text{CcCRE}) = E_{CBS(TQ5)} + (E_{MT(core)} - E_{MT(valence)}) + (E_{DK(rel)} - E_{DK(norel)}) + (E_{CCSDT/TZ} - E_{CCSD(T)/TZ}). \tag{7}$$

Additionally, the ACPF term is dropped and replaced with a CCSDT/TZ computation. The ACPF computations are the most costly, as are the CCSDT, but the latter is a reduction in cost over the former. Even so, the "E" term in HOCO shifts the frequencies upon its

inclusion both positively and negatively from the CcCR values upon its inclusion and only shifts the frequencies by typically ~ 1 cm^{-1}, 4 cm^{-1} at the most. In fact, the ν_2 C=O stretch at 1852.567 cm^{-1}[64] is actually more accurate with the CcCR QFF VPT2 approach than CcCRE QFF VPT2. The CcCRE QFF VCI ν_1 O−H stretch at 3634.4 cm^{-1} is exceptionally close to the gas-phase experimental value at 3635.702 cm^{-1},[65] on the other hand. Even so, the computational cost and inconsistency of the E term in either form has led to its omission from most of the subsequent QFF computations.

With the maturity of the CcCR approach, the anharmonic fundamental vibrational frequencies for a large number of molecules with astrochemical significance have been able to be computed. Some had existing experimental data, some did not, but none had a complete set of fundamental vibrational frequencies provided to the level that the CcCR approach could accomplish. These are given in Table 1.

While this list appears to be long, it represents over eight years of work. This highlights the fact that the CcCR method, even without the E term, is still exceptionally time consuming. While computer hardware has progressed over the preceding decade, the original trans-HOCO QFF energy point computations for 743 points and seven energies at each point required over 20,000 CPU hours. While more contemporary hardware could likely reduce this by several factors as can distributed computations, high-performance computer clusters, and even cloud computing,[109,127] the fact remains that a simple tetratomic molecule still requires an inordinately large amount of computer time to produce spectroscopic accuracy, which is nearly achieved for the CcCR QFF.[41] However, larger molecules, potentially with tens of thousands or even millions of points, are the next frontier in computing molecular vibrations of astrochemically-relevant species.

Explicitly Correlated QFFs

The advent of explicitly correlated wave functions[128] and their modern incarnations like the F12b formalism in CCSD(T) is a promising avenue in moving QFF technology forward.[129,130]

Table 1: Molecules Analyzed via CcCR QFFs to Date.

cis-$HOCO^{\cdot/-}$	Ref. 66	cis- & trans-HNNS	Ref. 67
$HOCO^{+}$ [a]	Ref. 68	$ArHAr^{+}$, $NeHNe^{+}$, $ArHNe^{+}$, $HeHHe^{+}$, $HeHNe^{+}$, & $HeHAr^{+}$ [d]	Refs. 69,70
$HOCS^{+}$	Ref. 71	HPSi & HSiP	Ref. 72
CH_2CN^{-}	Ref. 73	$NS_2^{\cdot/-}$	Ref. 74
l-C_3H^{+} [75b]	Ref. 76	c-CNN, c-CNC^{-}, c-$HCNN^{+}$, and c-N_3^{+}	Ref. 77
C_3H^{-}	Ref. 78	HOSO	Ref. 79
$NNOH^{+}$	Ref. 80	$CH_2NH_2^{+}$ [f]	Ref. 81
cis- and *trans*-HOCS and HSCO	Ref. 82	MgO, Mg_2O_2, $MgCH_2$, MgH_2, & MgF_2	Refs. 83–85
protonated acetylene ($C_2H_3^{+}$)	Ref. 86	cis- & trans-$HSSH^{+}$ as well as SSH_2^{+}	Refs. 87,88
c-C_3H^{-}	Ref. 89	c-SiC_2H_2	Ref. 90
NeH_2^{+} & ArH_2^{+} [c]	Ref. 91	H_2S^{+}	Ref. 92
ArH_3^{+}, $Ar_2H_3^{+}$, & $Ar_3H_3^{+}$	Refs. 93,94	$ArCH_2^{+}$ & $ArNH_2^{+}$	Refs. 95,96
$CCOH^{-}$	Ref. 97	$:CNH_2^{+}$ & $:CCH_2$	Ref. 98
$OCHCO^{+}$, $NNHNN^{+}$, NN-HCO^{+}, & CO-HNN^{+} [d]	Refs. 99–102	oxywater cation (H_2OO^{+})	Ref. 103
$SNO^{\cdot/-}$ & $OSN^{\cdot/-}$	Ref. 104,105	$NCNCN^{-}$ ($C_2N_3^{-}$)	Ref. 106
C_3P^{-}	Ref. 107	Isomers of [Al,N,C,O]	Ref. 108
$SiCH^{-}$	Ref. 109	c-$C_2NH_2^{+}$	Ref. 110
$ArOH^{+}$, $NeOH^{+}$, $ArNH^{+}$, $NeCCH^{+}$, $ArCCH^{+}$, $ArCN^{+}$, & $NeON^{+}$ [e]	Refs. 111–114	OAlOH, AlOH, & HAlNP	Refs. 115,116
HOX and HXO, X = Si^{+}, P, S^{+}, and Cl	Ref. 117	HCCOH	Ref. 118
SPSi	Ref. 119	HSO_2	Ref. 120

[a] Known in the ISM.[121,122]

[b] Claimed[123] and later confirmed as an interstellar molecule in the Horsehead nebula.

[c] Following from detection of ArH^{+}.[124]

[d] These are collectively called proton-bound complexes.

[e] The $ArOH^{+}$ computations informed later experimental observation of this molecule.[125]

[f] Later observed experimentally.[126]

This approach effectively reduces the size of the basis set necessary to reach the effective CBS limit and, in turn, likely the number of energies needed to be compute at each QFF energy point. The earliest exploration into explicit correlation for computing CCSD(T)-based QFFs of molecules with astrochemical significance is largely coincident with the earliest versions of the CcCR QFF.[131] A usual suspect list of H_2O, N_2H^+, NO_2^+, and C_2H_2 were explored with emerging R12 flavors of explicit correlation over a decade ago. In the case of the first three molecules, CCSD(T)-R12 performed as well as or slightly worse than the CCSD(T)/CBS results. However, the previously documented out-of-plane bending issues in C−C multiply bonded systems[40,132–134] was seemingly minimized with the R12 treatment. Such behavior produces erroneous and non-physical imaginary harmonic frequencies, among other issues, for certain levels of theory (MP2/aug-cc-pVDZ for example), but this is, again, reduced for explicitly correlated methods. However, at the time, the explicitly correlated methods alone were not enough to provide accuracies akin to those that CcCRE had begun to provide as the R12 approach being used was not sufficient for explicitly including core correlation. Even so, such approaches have crept into usage recently due to the huge cost savings in total computational time.

Specifically, CCSD(T)-F12b/cc-pVTZ-F12 (called F12-TZ from hereon) QFFs have been explored more recently in order to see if the computational cost can be reduced. In fact, they can. In a study comparing more than 20 molecules' worth of fundamental vibrational frequencies between CcCR and F12-TZ, the explicitly correlated method differs by less than 5 cm^{-1} typically.[135,136] The rotational constants do not fair as well, but the small shifts between F12-TZ and CcCR frequencies are often hovering around the available experimental data. Additionally, the reduction in computational time is on the scale of multiple orders of magnitude! As a result, this has opened the use of QFFs to even larger molecules beyond six atoms in some cases. Notable results are listed in Table 2.

In addition, core electron correlation can now be included in explicitly correlated computations. Work in this area has shown that computing CCSD(T)-F12b/cc-pCVTZ-F12 QFFs

Table 2: Molecules Analyzed via F12-TZ QFFs to Date.

Mg_2F_4	Ref. 85
c-(C)C_3H_2	Ref. 137
CH_2ClH^+	Ref. 138
CO_3 & C_2O_3	Ref. 139
$MgSiO_3$	Ref. 140
c-(CH)$C_3H_2{}^+$	Ref. 141
cis- & trans-HCSH as well as H_2SC	Ref. 142
SiO_2, SiO_3, Si_2O_3, & Si_2O_4	Ref. 143
ammonia borane (BH_3NH_3)	Ref. 144
AlH_2OH, HMgOH, AlH_2NH_2, & $HMgNH_2$	Ref. 145
AlH_3OH_2, SiH_3OH, & SiH_3NH_2	Ref. 146

slows down the computations and may or may not increase the accuracy.[147] However, this initial examination was only on inorganic oxide dimers of the form $(MO)_2$ where M = Mg, Al, Si, P, S, Ca, and Ti, and these may have properties unique from molecules comprised of typical upper-*p*-block atoms and hydrogen. Regardless, in this case the core correlation is treated within the single energy (and not as a composite correction term). The vibrational frequencies are nearly always less than valence F12-TZ by an average of 3.5 cm^{-1}. These are typically closer to the corresponding CcCR values but slow down the computations by a factor of roughly 13 in this case. However, the fewer core electrons in C, N, and O compared to S, Ca, and Ti will likely reduce this cost in lighter elements. Work is currently ongoing in this area, but promising results are on the horizon.

Small Molecules in Excited Vibrational States

Rotational spectra of vibrationally excited states have been observed in circumstellar and interstellar media, most notably for the C_6H radical[148] and SiS.[149] Similarly, acetylene,[150] carbon dioxide,[151] the C_{60} & C_{70} buckyballs,[152] and a few other molecules lacking dipole moments have been directly observed vibrationally and/or rovibrationally, as well.[153] Consequently, the rotational constants of vibrationally excited states are also useful reference data from quantum chemical computations as well as the combination bands and overtones,

especially for common astrochemical molecular species.

In every instance mentioned above in Tables 1 and 2, the CcCR QFF provides the zero-point averaged rotational constants, but these only require cubic terms. This is also true for being able to compute the vibrationally-averaged rotational constants for all of the fundamentals, as well as other excited vibrational states.[154,155] Hence, these values fall out of the QFF VPT2 computations within SPECTRO. These have been reported for nearly all of the molecules listed in the previous section.

However, other notable examples still remain. Foremost is SiC_2. This molecule has been observed toward the carbon-rich star IRC+10 216[156] as has the triatomic inverse of CSi_2 (SiCSi)[157] implying a diversity of carbon-silicon chemistry. The ν_3 antisymmetric Si−C stretching frequency in SiC_2 is computed[158] and experimentally-known[159] to be exceptionally low in frequency at 196.37 cm^{-1}. Hence, this mode can be thermally excited implying that overtones and combination bands would serve as a possible thermometer in regions where SiC_2 has been previously detected.[158] The first overtone lies at 507.7 cm^{-1} with $3\nu_2$ at 701.0 cm^{-1}. Even though VPT2 slightly underreports the associated vibrational frequencies, empirically-scaling the known rotational constants with with those computed for the excited vibrational states allows for what should be accurate semi-empirical rovibrational data provided for this potential molecular thermometer.[158]

Small Molecules in Excited Electronic States

While most of the molecules uniquely detected in various astrophysical media have come from radioastronomical observation with the next-most originating with infrared observation, some have come from detection of electronic spectral signatures.[153] Most notable is $C_{60}{}^+$[160,161] and its correlation with several of the diffuse interstellar bands, a series of unattributed UV-to-near-IR absorption features whose provenance is still nearly a complete mystery after more than a century.[162–168] However, the first three molecules observed beyond our Solar System were also detected from their UV-Visible spectra towards the star ζ Ophi-

uchi in the 1930s and 40s: CH, CN, and CH^+.[165,169–171] Additionally, the electronic spectral features of other small molecules are of notable importance for planetary and cometary observations within our solar system[172–176] making fully rovibronic spectral characterizations necessary for such molecules.[177]

The easiest way to treat molecular vibrations of electronically-excited states with QFFs is not to treat them as electronically-excited at all. Variationally-accessible and/or the lowest energy spin states different from the ground electronic state require no additional treatment beyond either standard CcCR or F12-TZ. This has been first implemented for CcCR QFFs with 1 $^3A'$ HCN, HNC, HCO^+, and HOC^+.[178,179] Additionally, the lowest quartet state of H_2SS^+[88] has been examined via QFFs and VPT2. The bent/linear electronic isomers of NS_2[74] along with the cyclic and bent electronic isomers of HC_2N[180] and HPSi/HSiP[72] have been computed in this manner, as well. The dipole bound excited states of CP^- and C_2P^-[181] have also been computed in a variationally-accessible ground state approach using specially constructed basis sets.[182] Even so, this is an exceedingly limited approach that requires an extremely narrow set of circumstance to be present in order to be useful.

A more generic approach would require moving beyond CCSD(T), though, in spite of its balance between accuracy and computational cost. Since CCSD(T) is a combination of an iterative CCSD method and a perturbational (T) correction, any electronic excitation method will be complicated. Within coupled-cluster theory, equation-of-motion (EOM) CCSD[183,184] is the standard excited state approach, but CCSD lacks the necessary correlation to produce highly accurate results for electronically excited states.[185] Other, approximate triples methods like CC3[186–188] are more accurate and produce wave functions open to electronic occupation shifts, but they are often exceedingly costly. There are more, exotic, triples-including, excited state coupled cluster methods, but none have thus far been able to garner a consensus among the community like CCSD(T) or even EOM-CCSD.

Hence, attempts have been made to compute QFFs based on EOM-CCSD with CC3 corrections. A CcCRE-like QFF has been constructed for 1 $^2A''$ HOC where this state

is actually variationally-accessible allowing for direct comparison to a trusted method in CcCR.[189] The so-called EOM-CcCE QFF energy is defined as:

$$E(\mathrm{EOM-CcCE}) = E_{\mathrm{CBS(TQ5)}} + (E_{\mathrm{MT(core)}} - E_{\mathrm{MT(valence)}}) + (E_{\mathrm{CC3/TZ}} - E_{\mathrm{CCSD/TZ}}) \quad (8)$$

with all terms implied to be for the same electronic state computed via EOM. This QFF has mixed results with the EOM-CcCE computations varying by as much as 25 cm^{-1} compared to the ground state CcC results.[189] While this use of explicitly computed anharmonic frequencies in electronically excited states is better than simple harmonics or even scaled harmonics, this method is not as accurate as would be desired compared to the ground state methods or even that which is necessary for comparison to laboratory astrophysical simulation. A refinement to this approach utilizing a scaling term from the ground electronic state in the difference in the CCSD-based CcCE QFF results and those from true CCSD(T)-based CcC (or CcCR) produces unobserved fundamentals for the excited 1 $^2\Pi$ state of the C_2H radical.[190] However, the errors are still on the order of tens of cm^{-1} for other known fundamentals and vibronic excitations. Again, even this approach is not as accurate as would be desired based on the performance of ground electronic state methods. Even so, a similar approach has been utilized in computing the 2 $^1A_1$ c-C_3H^- dipole bound state,[191] but problems in the electronic structure of the C−C antisymmetric stretching coordinate have led to only the a_1 and b_1 modes being reliably produced.

A recent breakthrough in this area has combined both CCSD(T) and EOM-CCSD in a novel way. This so-called (T)+EOM approach computes both the "ground state" (T) energy and the "excited state" EOM-CCSD energy and adds both to the CCSD energy[192] and is visually depicted in Figure 1. More precisely:

$$E_{\mathrm{(T)+EOM}} = E_{\mathrm{CCSD}} + E_{\mathrm{(T)}} + E_{\mathrm{EOM-CCSD}}, \quad (9)$$

where E_{CCSD} is the total reference and correlation energy up to the CCSD level, $E_{\mathrm{(T)}}$ is

Figure 1: A Visual Depiction of How the Excited State (Ψ_{XS}) is Accessed for Computing QFFs via the (T)+EOM Approach.

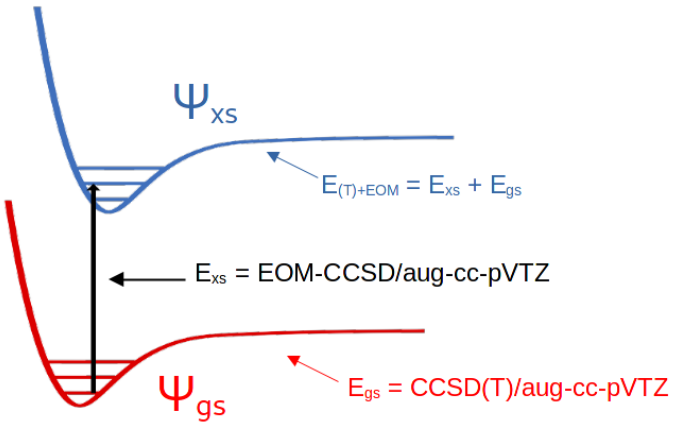

just the (T) contribution to the energy, and $E_{\mathrm{EOM-CCSD}}$ is only the excitation energy. In so doing, (T)+EOM/CcCR QFFs can be created that are equivalent in energy to those determined in Equation 7 with the appropriate terms included. For the sample set of HOO, HNF, HNO, and HCF species with variationally-accessible excited states, (T)+EOM/CcCR and standard CcCR often agree to better than 1 cm^{-1} and (with one exception) as far as 12 cm^{-1} for an average difference of less than 7 cm^{-1}. The one exception is the ν_2 bend in HOO, but the F12-TZ and (T)+EOM/CcCR QFF frequencies agree to better than 2 cm^{-1} at 1195.1 cm^{-1} implying that CcCR itself may be in error for this mode.[192] In any case, the (T)+EOM/CcCR method is currently being pushed and tested for new molecules in order to ascertain its robustness, and other excited state methods for computing QFFs are under development in order to provide fully rovibronic spectral data for molecules of astrochemical interest.

Large Molecules in Their Ground Electronic States

PAHs, buckyballs, and large carbonaceous molecules are believed to contain most of the carbon in the Universe not already tied up in CO or CO_2. Some estimates put this as high as 20% of all carbon atoms.[58] These also likely serve as reservoirs for the carbon observed in other small molecules potentially even those with astrobiological significance. With the

confirmed detections of benzonitrile, cyanonaphthalene, and even indene[193–196] in addition to earlier reports of benzene from IR observations,[197] there is now no doubt of PAHs existing in astrophysical environments. Even though some PAHs have small dipole moments, or functionalizing them clearly increases them, most PAHs will have negligible dipole moments if any at all. Hence, IR detections of PAHs are the most viable means of observing this entire class of molecules. The molecular vibrational and anharmonic fundamental frequencies are now needed more than ever if methods can be brought to bear to compute these values for comparison.

The largest CCSD(T)-based QFF produced to date has been on a mere eight atoms for ammonia borane.[144] The issue with going to larger molecules is that the number of points scales geometrically with the addition of each atom even for the sparsity of the PES provided by the QFF. While, again, explicitly correlated methods can reduce the computational cost of each point and higher symmetry molecules like those with a D_{2h} point group can in some ways reduce the number of points and the cost of each point, moving beyond 10 atoms requires moving beyond the safety of CCSD(T) and *wave function* based methods. While benzene could be computed with F12-TZ due to its high symmetry requiring "only" somewhere around 22,000 points for the QFF, most astronomers do not consider this molecule to be a PAH (since it's mono- and not polycyclic). That moniker for some does not appear until the seven rings of circum-benzene, or coronene, are present in the molecule. Coronene requires more than one million QFF points. For larger systems like PAHs, other methods must be employed.

Density functional theory (DFT) is really the most viable means of computing energies for placement into QFFs for subsequent VPT2 analysis. While various flavors of DFT fail inexplicably at times, this approach is the only one that steps beyond the Hartree-Fock approximation with enough accuracy to give hope for providing somewhat meaningful descriptions of molecular vibrations. One approach is to take DFT harmonic computations and scale them.[198–200] Such a methodology has even provided molecular vibrational data for

molecules with up to 384 atoms.[201] However, such methods cannot compensate for inconsistent anharmonicities or, most notably, treatment of vibrational resonances like QFFs and VPT2 can.[202] As a result, recent work has shown that DFT-computed QFFs can provide this, if the proper functional and basis set can be chosen.

Figure 2: Full IR spectrum of anthracene calculated using two methods, harmonic (top) and anharmonic (this work) (middle), compared with gas-phase spectra at 300 K (bottom). A selected region is shown with the relative intensities increased by a factor of five; from Ref. 203.

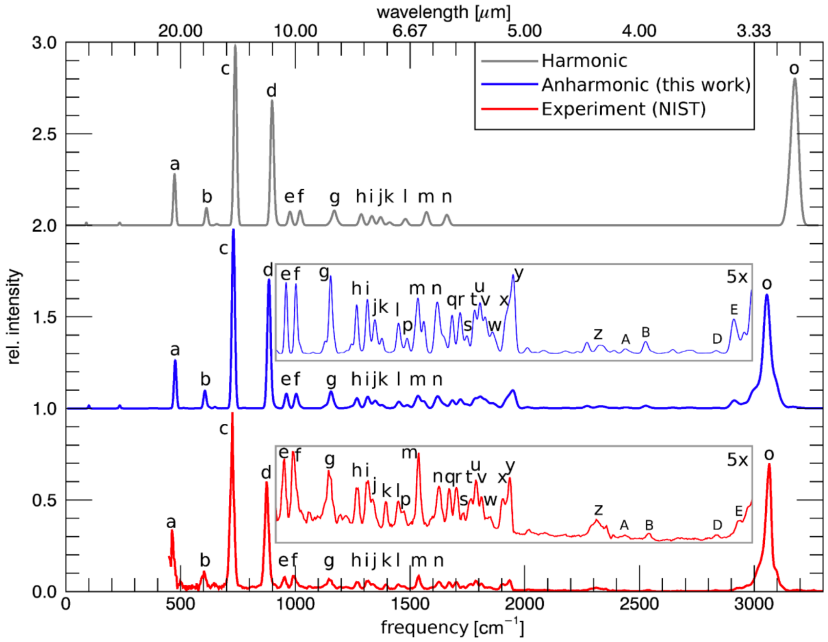

The first PAHs examined via QFFs and VPT2 include the linear acene family: naphthalene, anthracene, and tetracene.[203,204] The B971 functional[205] coupled to the TZ2P basis set gives accurate results for decent computational time cost even with the added tight convergence requirements. The QFFs are displaced via normal mode coordinates, which necessitates an initial computation of the harmonic vibrational frequencies. The double-harmonic intensities are also computed at this same level of theory. VPT2 from SPECTRO differs from that available in Gaussian16[206] mostly in that the resonance treatment, specifically coupling of symmetry-blocked Fermi resonance polyads for a limited energy range, are available. The utilization of resonance treatment produces fundamentals, overtones, combi-

nation bands, and their intensities − including the ability to describe intensity borrowing more completely within the polyad − all corrected for the resulting frequency shifts giving exceptional accuracy compared to experiment from the same work.[203,204] Some QFF VPT2 anharmonic fundamental vibrational frequencies agree to experimental precision. Others vary by ~ 10 cm^{-1}. The visual spectra, though, are nearly indistinguishable between theory and experiment in this case as shown in Figure 2 for anthracene, taken from Ref. 203. Such is not true for the harmonic spectra, scaled or otherwise, largely due to the lack of resonance treatment. With so many vibrational frequencies in such a high density, the resonances are essential for proper treatment of the vibrational/IR spectrum.[203]

This work has been followed by similar analysis of larger PAHs including benz[a]anthracene, chrysene, phenanthrene, pyrene, and triphenylene[207] as well as the methylated PAHs 9-methylanthracene and 9,10-dimethylanthracene in addition to the hydrogenated PAHs 9,10-dihydroanthracene, 9,10-dihydrophenanthrene, 1,2,3,4-tetrahydronaphthalene, and 1,2,3,6,7,8-hexahydropyrene.[208] The inclusion of the aliphatic groups in the latter study further informs correlation between theory and experiment where isolation of pure PAHs is nearly impossible. The visual spectra are once again nearly indistinguishable for the substituted PAHs, and the accuracies are good. However, some errors creep into the results for a few of the C−H stretches and in some of the intensities.[208] While such results are still wildly successful, the aliphatic contributions are more in error than the aromatic frequencies. This result implies that one DFT functional cannot be applied to all molecules for a reduction of computational cost. B971/TZ2P works exceptionally well for PAHs, but, while still good, is not as predictive for aliphatics leading to use of B3LYP[209–211] with the double-ζ N07D basis set[212] in such cases.[208] Hence, more refinement in the choice of methods will be required for moving into functionalized PAHs. Even so, the use of B971/TZ2P QFFs with resonance-treated VPT2 is promising for advancing the study of molecular vibration spectra for PAHs.

A major remaining issue for the QFF computations of large molecules is that anharmonic DFT still is not tractable for the computation of coronene-level PAHs or larger. The density

of IR bands likely arising from PAHs and related species is virtually optically opaque in some regions,[213,214] and the diversity of possible PAHs, including those with aliphatic portions, becomes an exercise in statistical probability and stochastic geometry. Consequently, computational methods are really needed to create trustworthy, but high-throughput spectral characterization into the astrochemical literature. Of course, work is ongoing in this area in order to produce meaningful, anharmonic vibrational spectra for larger PAHs.

Computing Rovibrational Line Lists for Eliminating "Weeds" and Providing Data for Modeling the Opacity of Exoplanet Atmospheres (Absorption & Emission)

QFFs provide sparse PESs that are relatively quick to compute. However, the accuracies begin to break down in moving beyond the fundamental vibrational frequencies and their corresponding rotational constants and spectroscopic data. A larger PES is required in order to provide the most accurate descriptions of the full rovibrational spectral values, also called rovibrational line lists. This usually involves a global PES. Even so, the two approaches have some similarities. Most notably, the principle energy computed at each point on the surface can be computed through any flavor of quantum chemical method desired. Some of the most accurate line lines are still based on the CcCRE energy with the ACPF "E" term included as defined above in Equation 7. Even for small molecules, such energies are costly on the scale of hundreds of thousands of points on the PES. Hence, lower levels of theory are often brought to bear initially in order to sample the PES geometries and select a subset of those that are required to represent a chosen energy range. Once the higher-level PESs are computed as informed by the lower level guidance, these PESs are then fit to very high tolerances. Refinement of the PES using known empirical parameters to very high accuracy serves to enhance significantly the accuracy of the line list, usually by ~ 3 orders of magnitude. This

has led to the Best Theory + Reliable High-Resolution Experiment (BTRHE) strategy and has produced line lists of notable accuracy for several molecules discussed below.[215] Other groups have provided similar line lists for similar astrochemical applications,[11,216,217] but the present discussion will largely focus on work from the NASA Ames group.

The selection of molecules for such line lists must be done with care as it may take years to produce a quality PES, empirical fit, variational computation, and even dipole moment surface (for the intensities) at a low enough noise level. As mentioned above, water is an obvious candidate.[218] Additionally, atmospherically-relevant species also are sensible for both terrestrial applications, exoplanetary considerations, and planetary modeling. This has led to the selection of CO_2, NH_3, and SO_2[15,215] for the other molecules thus far examined via such high-level analysis. Hence, these molecules will be present across all spectral ranges not just the ones in which they have previously been detected. This implies that they will exhibit unknown transitions even though they are known molecules. These may be overtones and combination bands but are much more often rotational lines of various vibrational quantum levels. Such spectral lines are called "weeds" since they do not add to the chemical inventory of a certain celestial body and often add little to the understanding of the underlying physical conditions. The only way to trim these "weeds" in order to find the "flowers" (the unknown transitions of unknown molecules) is to provide highly accurate line lists for common molecules and remove them from the observed astronomical spectra.

Another important application for these highly accurate rovibrational line lists is modeling the opacity of planetary atmospheres, especially exoplanets.[219] The study of exoplanets, planets outside our solar system, has exploded in recent years and the next phase of these studies will be to characterize the atmospheres of exoplanets to determine their nature, and ultimately whether they may be able to support life. In the near term, JWST will most likely be used to characterize the atmospheres of the closest known exoplanets, and many of these are very hot, approaching 2000 K or more. Hence the rovibrational line lists for the molecules discussed here need to be highly accurate, but also extend to very high rovibrational energies

in order to cover the appropriate temperature range.

Small, Stable, Abundant Molecules: CO_2

The first PES produced for CO_2 is isotopic-independent with a root-mean-squared (RMS) error compared to known experimental lines of 0.0156 cm^{-1} for 6873 $J = 0-117$ transitions for the principle isotopologue.[220] The isotopologues increase the RMS by an order of magnitude, but this is still a small error. The initial dipole moment surface (DMS) is able to produce intensities to within 20% of the experimental values providing a useful high-resolution benchmark for subsequent analysis at or below 296 K.[220] A CCSD(T)/aug-cc-pVQZ DMS is able to refine the accuracy of the intensities and further increasing the J values up to 150 and the temperature up to 1000 K.[221]

Figure 3: Measured 5001r-00001 (r=3, 4) line positions and intensities, compare to Ames-296 K line list and Wattson 750 K (also called High-T or HOT-CO_2) line list; from Ref. 221.

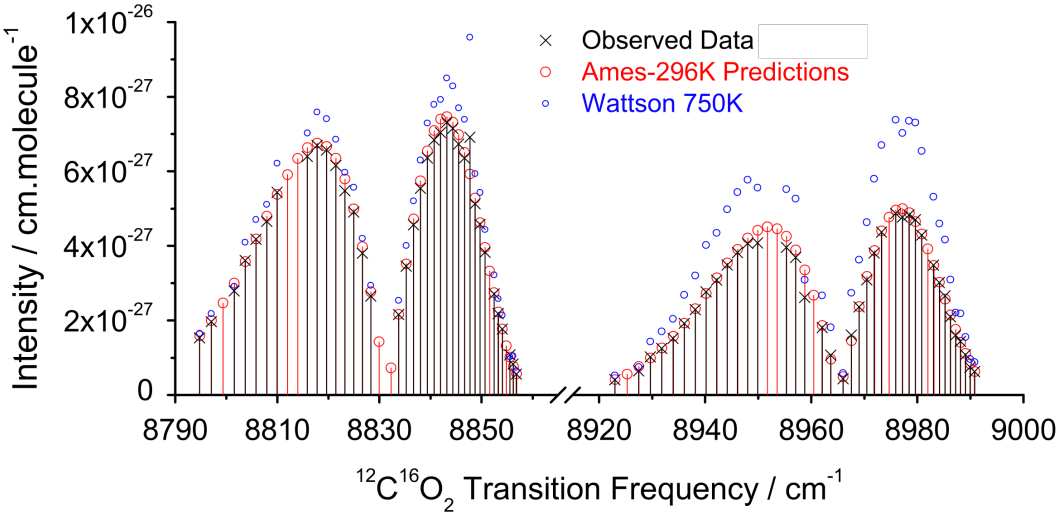

Additional refinements allow the PES for all 13 major (and some minor) isotopologues of CO_2 to stretch up to 18,000 cm^{-1} and 1500 K while also providing line shapes for planetary bodies including the Earth but also Mars and Venus with hotter conditions possible.[222] Line accuracies at such higher energies are better than 0.05 cm^{-1} implying a well-suited description of the line lists for unknown transitions. In addition, problems in existing experimental

data have been identified as demonstrated in Figure 3 (Figure 2 from Ref. 221). In this figure, excellent agreement between the Ames line list and recent experiments for two specific rovibrational bands is found for both line positions and intensities, while the HITRAN2008 intensities are two orders of magnitude too low. While studies of CO_2 reach into the 1500 K range, planetary conditions of Venus, hot Jupiter exoplanets, and circumstellar envelopes will extend beyond this temperature range requiring higher energy line lists. Hence, this line list is performing exceptionally well at these higher temperatures and can be usefully extended even further up the temperature scale in order to provide even more rovibrational lines for CO_2 and its isotopologues.[223,224]

In the latest DMS computed for CO_2, intensities are now predicted to within a few percent for some strong bands but at least to within 90% of experiment.[224] In fact, new experiments are actually needed at this point because the possibility remains that the computations are more accurate than the current experiments. Additionally, computing accurate rovibrational line intensities requires accurate total internal partition sums (TIPS), also called internal partition functions, and the Ames CO_2 and isotopologue line lists have been used to yield very accurate TIPS.[225]

Small, Stable Molecules with Large Amplitude Motions: NH_3

Not all molecules lend themselves to straightforward study, however. The barrier to linearity in water is relatively high at more than 11,000 cm^{-1},[226,227] but the inversion barrier, the so-called "umbrella" motion, of ammonia is much lower at roughly 2,000 cm^{-1}, below many of the fundamental vibrational frequencies. While such features can play havoc on a QFF at times,[41] the global PES required for line lists can, if treated properly, alleviate these concerns in many ways.[15] Granted, the proper choice of coordinates for a QFF can also circumvent these issues, specifically including NH_3,[18] but not in all cases.[94,99] Regardless, ammonia is known to exist in interstellar regions,[228] protoplanetary disks,[229] planetary atmospheres,[230] and other astrophysical regions. While not as common as water, this simple hydride plays a

vital role in many astrochemical pathways requiring the most accurate of computations for comparable results.

Figure 4: 2 orders of magnitude rms error reduction from HSL-0 to HSL-1 to the latest HSL-2. From left to right, (a), (b), and (c) are for HSL-0/1/2, respectively; from Ref. 231.

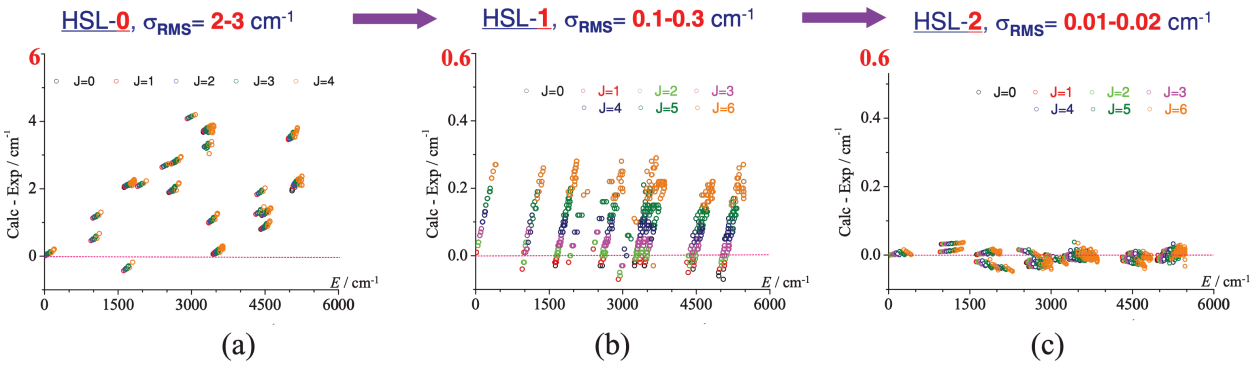

The first highly accurate line list for NH_3, again, utilizes the CcCRE-type (Equation 7) energy with ACPF sometimes and sometimes not included as well as diagonal Born-Oppenheimer corrections.[232] The initial fitting for the $J = 0 - 2$ bands gives a RMS compared to 13 database benchmarks of 0.023 cm^{-1}, and these do not reduce for theoretical benchmarks past 10,000 cm^{-1}. The inversion is computed to be 1784.19 cm^{-1} within 3 cm^{-1} of previously computed values.[232] The ammonia line list is further corrected utilizing a second-order correction for the Born-Oppenheimer approximation and additional experimental refinements.[231] Figure 4 (Figure 3 from Ref. 231) shows how the NH_3 PES improves by two orders of magnitude from purely *ab initio* (HSL-0), to initial refinement (HSL-1), to refinement and inclusion of non-adiabatic Born-Oppenheimer breakdown terms (HSL-2). Additionally, the HSL-2 PES is used to compute the purely rotational transitions for $^{15}NH_3$ and compare to the Cologne database,[233] and the RMS error is a mere 0.00034 cm^{-1}. Further, a deficiency of the $^{15}NH_3$ rovibrational energy levels is identified and tied to a problem with an effective Hamiltonian model used to fit the experimental data.[231] As a result, the accuracy of the PES opens the possibility for exploring existing, unassigned HITRAN data. Strong mixing between the $2\nu_4$ overtone and the $2\nu_2 + \nu_4$ combination bands shows to be the

source of deficiencies in the experimental modeling of $2\nu_4$, and new predictions of the $4\nu_2$ band and its associate lines result from this analysis.[234] Building upon this notable strength of the ammonia line lists, comparison to experiment has been able to elucidate the origins for several hundred spectral features including nearly 4800 NH_3 positions and intensities between 6300 cm^{-1} and 7000 cm^{-1} providing unprecedented clarity for such higher-order transition lines.[235]

Small, Stable Molecules Containing a Heavy Atom: SO_2

Figure 5: Ames-296K list based IR simulations (Top) vs. experimental spectrum analysis (Bottom). Discrepancies between the Ames analysis and the reported experimental assignments are as obvious as the very good agreement. $\sigma = 0.001$ cm^{-1} in the Ames Guassian convolution; from Ref. 236.

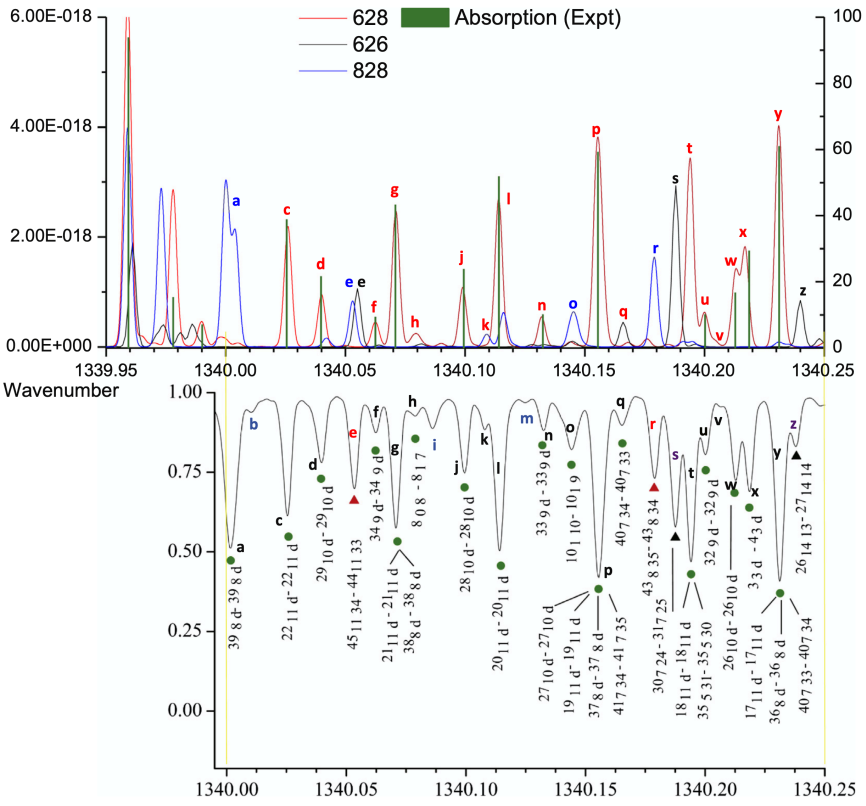

The lessons of both ammonia and carbon dioxide also serve in the line list creation for SO_2. Sulfur dioxide is of notable significance for the Venusian atmosphere[237] especially in the sulfuric acid cycle[238] and the interstellar medium[239] among other sources. Its study

also builds off of the approaches refined from the other two molecules from the NASA Ames group discussed above and can be found online (`http://huang.seti.org/`). The BTRHE approach for this molecule begins with a CcCR PES, a CCSD(T)/aug-cc-pV(Q+d)Z DMS, and an empirical fitting to HITRAN data.[12] The lines fit for SO_2 at 296 K cover up to 5,500 cm^{-1}, have uncertainties of less than 0.03 cm^{-1} per each line, and produce intensities to within 15% or better of experiment, though the line list is likely to be reliable up to about 8000 cm^{-1}. within 15% of experiment. Extension of the PES to the $^{32/33/34/36}S$ and ^{18}O isotopologues perform similarly well as the standard isotopologue.[240] Additional work in conjunction with the ExoMol group from the University College London has been able to produce a whopping 1.3 billion lines for temperatures up to 2000 K giving incredibly fine grained results for a more complete line list of SO_2.[241] The refined $^{32}S^{16}O^{18}O$ line list also provides alternatives for questionable empirical assignments and experimentally missing bands.[236] As shown in Figure 5 (Figure 6 from Ref. 236), assigning experimental rovibrational lines for $^{32}S^{16}O^{18}O$ can be difficult because there will also be lines from the pure $^{32}S^{16}O_2$ and $^{32}S^{18}O_2$ isotopologues. Consequently, those need to be assigned first, whereas such problems do not exist for the computed rovibrational line lists. Extension to the $^{32/33/24}S^{18}O_2$, $^{32}S^{18}O_2$ and $^{16}O^{32}S^{18}O$ isotopologues largely completes the 296 K lines for all notable versions of sulfur dioxide.[13,224] Further refinement for SO_2 will require additional high-resolution rovibrational experiments that go above 8000 cm^{-1}, as well as high-resolution rotational experiments that include "hot" microwave transitions, i.e. transitions from excited rotational levels.[242] Even so, the line lists in these regions based on PESs fit to the lower temperature and lower energy data can serve as an initial guide for future experimental analysis, as has already been the case.

The goal for such line lists still remains two-fold: a) to provide a means of removing the unknown transitions of known molecules, and b) to provide data for modeling the opacity of planetary atmospheres, especially exoplanets. While CO_2, NH_3, and SO_2 (in addition to water)[216,218,227] represent a small sample of notable species, they have a huge potential impact

on the regions where they are present. Hence, removal of their spectral features is key in finding new molecular species hidden among their lines. Additionally, other molecules' line lists have been computed by the ExoMol group (`https://www.exomol.com`), the Reims-Tomsk group (`http://theorets.tsu.ru`; `http://theorets.univ-reims.fr`), and even more rovibronic spectral data are currently being proposed to the community.[177] Future directions will include potential bio- and even technosignature molecules where the density of lines can serve as definitive evidence for such molecules beyond a few features (or even just a single feature as has been claimed recently for phosphine[243]). Consequently, the BTRHE approach as well as CcCRE PES data will continue to inform future work in producing line lists for astrochemical "gardening" in pruning "weeds" in search of "flowers."

Simulating Cascade Emission Spectra of Large PAH Molecules (Emission)

Most of the astrochemistry vibrational and rovibrational spectroscopy discussed earlier involves predicting the absorption spectroscopy of small or even large molecules for comparison to either astronomical observations or laboratory experiments. The one exception is modeling the opacities of (exo)planetary atmospheres as the astronomical observations will be of the emission coming from these (exo)planetary atmospheres. In that case, however, the line lists are so complete that computing the density of states reliable, and, subsequently, the opacity computations are relatively straightforward, even if computationally intensive. Trying to simulate the IR emission spectra from astronomical observations of the interstellar medium (ISM), circumstellar shells, or other low-density astrophysical environments is wholly different, though. In such environments, the emission spectrum is dominated by bands that were originally referred to as the unidentified infrared bands (UIBs or, equivalently, UIRs), but are now commonly referred to as the aromatic infrared bands (AIBs).[244–246] The AIBs are widely believed to emanate from emission of relatively large PAH molecules (ca. 50 carbon

atoms).[244]

The astrophysical environments from which the AIBs originate are harsh and generally have a large flux of ultraviolet (UV) photons due to the presence of nearby stars. Hence, small molecules are readily photodissociated and do not survive. Large PAH molecules, on the other hand, can absorb even a 12 eV photon and survive provided the excess energy is radiated away before absorbing another such photon.[244] The mechanisms behind this are straightforward: a) a UV photon is absorbed, exciting the large PAH molecule into an excited electronic state; b) the large PAH molecule reverts to the ground electronic state due to non-adiabatic coupling with the excess energy then deposited into molecular vibrations; c) because the large PAH has so many vibrational degrees of freedom and due to the density of states, most individual vibrational degrees of freedom will not have very much energy deposited into them; d) this gives the molecule time to start emitting IR photons; e) after each photon is emitted, the excess energy in the molecule is redistributed due to intermolecular vibrational relaxation (IVR); and, finally, f) steps d) and e) continue until the PAH molecule is once again in its ground vibrational state, which is referred to as a cascade emission spectrum.[244,247] The PAH molecule is then ready to absorb another UV photon and repeat the process. The time scale for steps b) and e) is very rapid $\sim 10^{-8}$ s or less, whereas the time scale for step d) is $\sim 10^{-6}$ s, and the time scale for the entire cascade spectrum is $\sim 10^{-3}$ s.[244] The challenge for us, then is to compute a simulated cascade emission spectrum of a large PAH molecule, and this cannot be done with, for example, a line list as the theoretical methods applied there are much too expensive to be used on a large PAH molecule. In the sections below, the most commonly used approach thus far is discussed, which makes use of scaled harmonic vibrational frequencies. However, a fully anharmonic vibrational frequency approach was developed only a few years ago and work on refining it continues presently.

Cascade Emission Spectra from Scaled Harmonic Frequencies

For this section, the model used in the NASA Ames PAH IR Spectroscopic Database (denoted PAHdb) is examined.[200,248–250] Several factors are considered including band position, band shape, line width, and relative band intensities. For the band position, since most anharmonic corrections are negative (i.e., lower a given transition energy), the highest energy photon that could be emitted for a given vibrational mode is known to correspond to the molecule relaxing from the first excited state for that mode to the ground vibrational state (the zero-point energy level). To see this, examination of the VPT2 vibrational energy level formulae for asymmetric tops[24,26,154,155,251,252] is useful:

$$E(\nu) = \Sigma_{k=1}^{N} \omega_k \left(\nu_k + \frac{1}{2}\right) + \Sigma_{k\leq l}^{N} X_{kl}(\left(\nu_k + \frac{1}{2}\right) \left(\nu_l + \frac{1}{2}\right) \tag{10}$$

where ω_k is the harmonic frequency of vibrational mode k, ν_k is the vibrational quantum number for mode k, and X_{kl} is the anharmonic constant connecting modes k and l. This is in many ways a reformulation of Equation 4 from earlier. Since the anharmonic constants are generally negative, as one moves to higher quantum numbers ν_k, the vibrational energy levels will become closer together. In a cascade emission spectrum, many of the emitted photons will not originate from the first excited vibrational state, and, therefore, the band position will be somewhat lower in energy than the fundamental. In order to approximate this effect using only scaled harmonic vibrational frequencies, the band positions can be shifted. This is probably most important for the C−H stretches because they have the largest anharmonic correction generally, and they will tend to emit more when the molecule is fairly energetic. That is, in the cascade emission process, the C−H stretching modes will be statistically less populated as the molecule emits more photons and its internal vibrational energy is reduced. In fact, near the end of the cascade emission process, the photons being emitted will almost all be the low energy vibrational frequencies that occur in the far-IR.[248,253]

The band shapes are generally taken to be either Lorentzian emission profiles or Gaussian

profiles, and there are arguments in favor of both.[254] The NASA Ames PAHdb has adopted a Lorentzian emission profile for individual PAH molecules as given by:

$$\mathcal{P}(\nu) = \frac{1}{\pi} \frac{\frac{1}{2}\Gamma}{(\nu - \nu_i)^2 + (\frac{1}{2}\Gamma)^2} \tag{11}$$

where $\frac{1}{2}\Gamma$ is the full width half max (FWHM) line width and ν_i is the scaled harmonic vibrational frequency of mode k.[248] The FWHM line width is allowed to be frequency dependent where the mid-IR range is given a FWHM of 10-30 cm^{-1}, while vibrational modes in the far-IR (in the 15-20 μm or 667-500 cm^{-1} range) are given FWHM values of between 4-8 cm^{-1}. When using the NASA Ames PAHdb to fit astronomical spectra using many PAH molecules, Gaussian profiles have been found to perform better in this situation.

Relative band intensities are obtained by multiplying the intrinsic band intensity by a blackbody at an average emission temperature or by using a somewhat more sophisticated model involving the specific PAH molecule's heat capacity. In Ref. 248, there are some details of the cascade emission process that are not described well enough to know for sure how the NASA Ames PAHdb handles them. For example, the cascade emission process is seemingly not followed explicitly, but, rather, it adopts a canonical description of the ensemble. Thus, the emission cascade is evaluated through a statistical mechanics approach, but details of this are not given, though some additional details are given in Appendix A of Ref. 255. Another consequence of using scaled harmonic frequencies is that the only vibrational bands with a non-zero IR intensity are the fundamental vibrational frequencies, and, thus, the density of states just ends up being the total number of fundamental vibrational frequencies. This winds up being a significant undercount for a large PAH molecule.

Fully Anharmonic Cascade Emission IR Spectra

In 2018, Mackie et al.[247] showed how to use the data from an anharmonic VPT2 analysis (including harmonic frequencies, anharmonic constants, and coupling terms used in the polyad

matrices) to create a fully anharmonic cascade emission IR spectrum of a PAH molecule, including the incorporation of polyad resonance matrices for fundamental vibrational frequencies as well as bands originating from excited vibrational states. This publication built upon their earlier work where VPT2 was applied to the IR absorption spectrum of a PAH molecule at low temperatures and then compared with high-resolution experiments in the C-H stretch region or low-resolution spectra covering most of the IR region (not much below ~ 500 cm^{-1}).[203,207,208,256,256,257] In the earlier works, the importance of including resonance polyads is demonstrated especially in comparing to the high-resolution experiments in the C-H stretch region, where very good agreement was found. In these studies, Mackie et al. use a DFT functional basis set approach to compute the QFF, wherein the combined DFT functional and basis set had been shown previously to yield reasonable results for larger molecules.[258,259] The incorporation of the polyads into the VPT2 analysis follows earlier work, as well,[202,260] but the method to distribute the IR intensities across the bands included in the polyads according to the eigenfunctions of the polyad matrix is novel.[203]

Modifying the VPT2 analysis for low-temperature IR absorption spectra to compute a cascade emissions spectrum, the exact type of spectra that astronomers observe, poses several new challenges. First, since the PAH molecules would have very high internal energies, i.e., be very hot, temperature dependent IR spectra for PAH molecules must be computed. This had previously been done for several PAH molecules in the context of IR absorption spectra, and in particular Mackie et al. adopt an approach using a Wang-Landau style walk, a Monte Carlo sampling method, that had previously been used in conjunction with QFFs for PAH molecules.[261–263] The first step involves using a Wang-Landau walk in order to estimate the vibrational density of states (DOS) required for a temperature dependent spectrum. Following the calculation of the DOS, a second Wang-Landau walk is used to compute an energy dependent spectrum. The full details will not be expanded here, but the interested reader is referred to Mackie et al.[247] for the details. One point to note, however, is that Mackie et al. have to modify the procedure slightly in order to compute the temperature

dependent emission spectra as opposed to the temperature dependent absorption spectrum. A second point to note is that Mackie et al. explicitly follow the cascade emission spectrum, reducing the internal energy in the PAH molecule once a photon is emitted, and allow for a redistribution of this internal energy via IVR using the DOS.

Figure 6: The effect of including polyads (blue, bottom panel) and excluding polyads (red, top panel) from the anharmonic temperature-dependent calculations of 9-methylanthracene using the Wang–Landau approach; from Ref. 247.

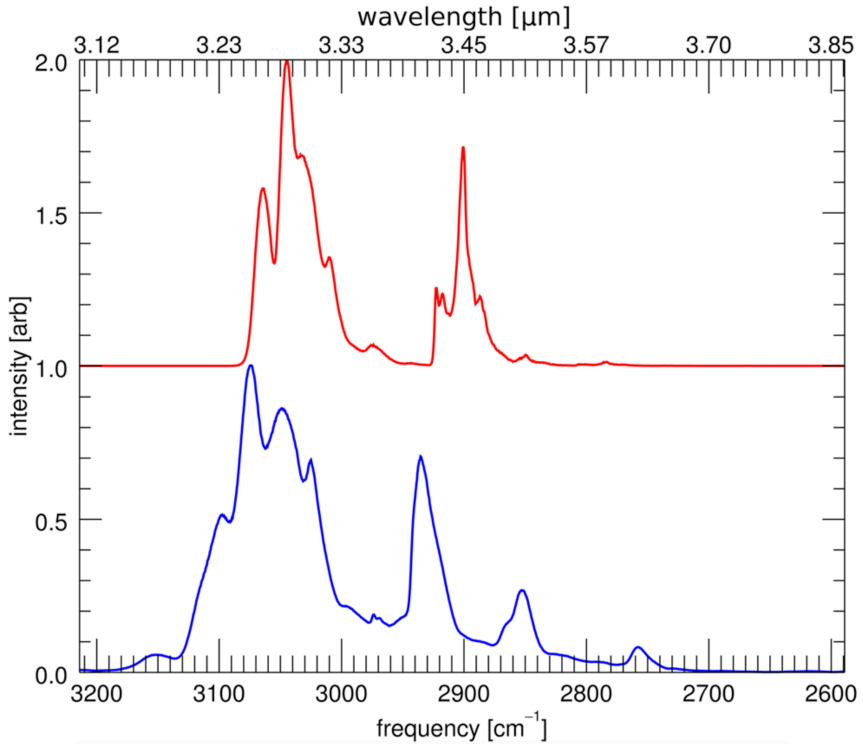

An important innovation introduced by Mackie at al. is to diagonalize the polyad matrices not just for the fundamental vibrational frequencies but also for excited vibrational frequencies. They point out that for excited vibrational frequencies, say for example the overtone of a C−H stretch, the states involved in the polyad are similarly excited by one quantum in the C−H stretch of interest. Since the underlying coordinate system used in VPT2 is the normal coordinates, they note that the polyad matrices are closely related. The off-diagonal elements only depend on the difference between the states so these matrix elements do not change, and only the diagonal elements change. Thus, the polyad matrices are

re-diagonalized for all necessary states, and, again, the IR intensity for the bands resulting from the polyad are distributed according to the eigenfunctions of the polyad diagonalization. To show the importance of including the polyads in temperature dependent spectra, Figure 1 from Mackie et al.[247] is reproduced here (Figure 6) where the blue spectrum has included polyads, and the red spectrum is where polyads are excluded for 9-methylanthracene. There is clearly a difference in these spectra, highlighting the importance of including polyads in the temperature dependent spectra. Further, Figure 2 of Mackie et al. (Figure 7 here) is reproduced as well, which demonstrates the importance of re-diagonalizing the polyad matrices for excited vibrational states. Spectra from several temperatures are given, and the importance of a particular combination band is shown and becomes more pronounced at higher temperatures.

Figure 7: The theoretical infrared spectrum of tetracene showing an increase in the relative intensity of a combination band (marked with an "*") as the internal temperature is increased; from Ref. 247.

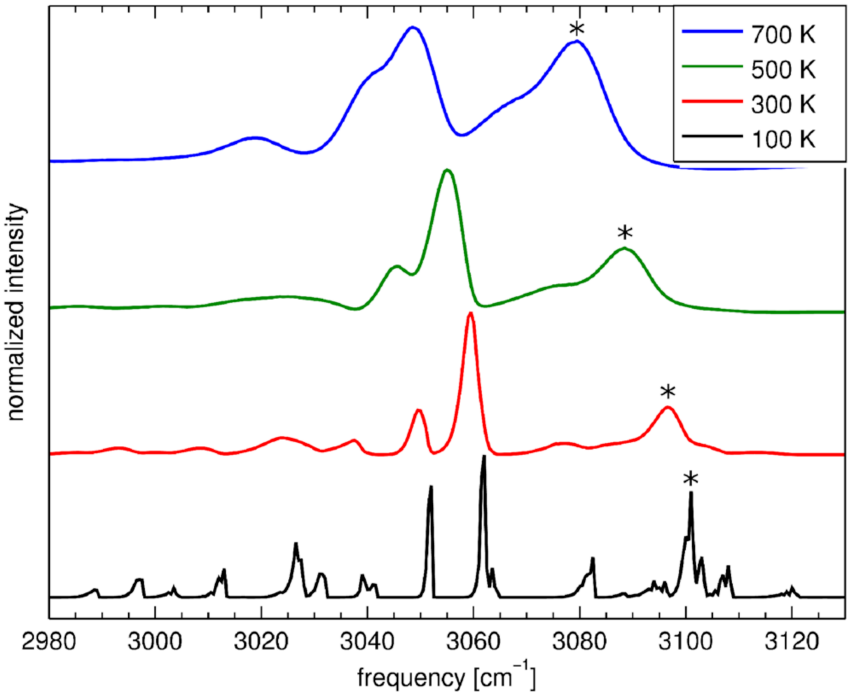

Several other important phenomena have been investigated in computing the cascade emission spectra of a PAH molecule, such as how a band profile changes with temperature

when there are two bands close to each other and how the cascade emission spectrum changes depending on the starting temperature (or energy of the absorbed UV photon). Mackie et al. also examine "snap-shot" emission spectra as opposed to a cascade emission spectrum, and, in a separate study, Chen et al.[264] show that an experiment conducted by Wagner et al. in 2000[265] is in fact a snap-shot emission spectrum of pyrene as opposed to a cascade emission spectrum. In the 2018 study, Mackie et al.[247] do not investigate the use of line-shapes, but more recently Mackie et al.[266] examine using Gaussian emission profiles together with the inclusion of rotational broadening for the 11.2 μm feature of anthracene, tetracene, and pentacene and how this affects the overall band profile. There is still much work to be done in order to determine the best line-shapes to use as well as the development of techniques which will allow QFFs to be computed for larger PAH molecules, and this work continues.

In this section, there are some important aspects that have not yet been addressed. Firstly, it is reasonable to ask whether VPT2 is applicable to highly excited PAH molecules. To see why this is the case, consider that a 12 eV photon will contain about 100,000 cm^{-1} in excess energy. However, the PAH molecules thought to exist in the harsh environments where they are observed by astronomers should contain 40-50 carbon atoms (various estimates exist, but this is on the low end),[247] which means that with the necessary hydrogen atoms to complete the PAH molecule, there will easily be more than 100 vibrational degrees of freedom. This implies that even with 100,000 cm^{-1} in excess vibrational energy, all of the energy could be accommodated with the average ν quantum number less than 1. Considering the density of states, clearly, in most instances, there will not be too much energy (i.e., large ν quantum numbers) in any one vibrational mode or degree of freedom. Hence VPT2 should perform well in these instances provided that the molecules are tightly bound and do not contain large-amplitude motions. Since PAH molecules, often referred to as 'chicken-wire' molecules, form a rigid molecular framework, there should not be large-amplitude motions. One exception to this is examining a PAH molecule with an aliphatic chain replacing a

hydrogen atom as in 9-methylanthracene. In these cases, Mackie et al.[208] just treat the vibrational degrees of freedom which exhibit a large-amplitude motion, such as the hindered rotation of the methyl group, at the harmonic level of theory. In general, however, PAH molecules are exceedingly well suited to be treated with VPT2 provided the large number of resonances are treated properly through polyads.

Conclusions

Quantum chemistry is uniquely suited to provide novel insights for molecular vibrations of molecules relevant to astronomical studies. Various astrophysical regions exhibit conditions too harsh or otherwise too difficult to replicate in the laboratory. Computational simulation is well-suited to provide data for molecules found in such regions if only the methods employed are accurate enough. This work shows that advanced electronic structure theory computations (like the CcCR composite approach) tied to rather straightforward vibrational methods (such as VPT2) can produce exceptional comparison to experiment. Such methods can then move beyond replication and on to prediction. The unique and novel vibrational, rotational, and rovibrational spectra data for more than 50 molecules have been produced within the past decade with benchmarks for such methods implying errors on the average of 7 cm^{-1} or less, and often much less. Additionally, development is currently moving beyond simply providing rovibrational spectral data for small molecules. Modern work is stretching electronic structure theory to compute relevant molecular vibration data for electronically excited states, ever-larger molecules, highly-accurate molecular line lists, and even full infrared cascade emission spectra. All of these studies are geared towards expanding the inventory of attributed astrophysical spectral features in numerous astronomical objects ranging from circumstellar envelopes to photodissociation regions to exoplanetary atmospheres and even to the diffuse interstellar medium. The computational results are now, in many ways, going hand-in-hand with experiment and, in some circumstances, beginning to show signs of

superseding it. Regardless, the volume of the throughput, granular nature of the results, and definitive descriptions of the simulated spectral features makes quantum chemistry well-placed to be a principle partner in the elucidation of molecular vibrations for molecules of astrochemical interest.

Acknowledgement

RCF is supported by NASA Grant NNX17AH15G, NSF Grant OIA-1757220, and startup funds provided by the University of Mississippi. TJL gratefully acknowledges financial support from the 17-APRA17-0051, 18-APRA18-0013, 18-2XRP18 2-0046, and NASA 20-EW20_2-0144 grants. Megan Davis of the University of Mississippi is acknowledged for providing Figure 1. Additionally, the authors would like to thank Dr. David W. Schwenke of the NASA Ames Research Center and Prof. Alexander G. G. M. Tielens of the Leiden Observatory for assistance in editing the manuscript.

References

(1) Turner, B. E. U93.174 - A New Interstellar Line with Quadrupole Hyperfine Splitting. *Astrophys. J.* **1974**, *193*, L83–L84.

(2) Green, S.; Montgomery, J. A.; Thaddeus, P. Tentative Identification of U93.174 as the Molecular Ion N_2H^+. *Astrophys. J.* **1974**, *193*, L89–L91.

(3) Tucker, K. D.; Kutner, M. L.; Thaddeus, P. *Astrophys. J.* **1974**, *193*, L115–L119.

(4) Guèlin, M.; Green, S.; Thaddeus, P. *Astrophys. J.* **1978**, *224*, L27–L30.

(5) Wilson, S.; Green, S. Theoretical study of the butadiynyl and cyanoethynyl radicals - Support for the identification of C3N in IRC + 10216. *Astrophys. J.* **1977**, *212*, L87–L90.

(6) Buhl, D.; Snyder, L. E. Unidentified Interstellar Microwave Line. *Nature* **1970**, *228*, 267.

(7) Herbst, E.; Klemperer, W. Is X-Ogen HCO^+? *Astrophys. J.* **1974**, *188*, 255–256.

(8) Nickerson, S.; Rangwala, N.; Colgan, S. W. J.; DeWitt, C.; Huang, X.; Acharyya, K.; Drozdovskaya, M.; Fortenberry, R. C.; Herbst, E.; Lee, T. J. The First Mid-infrared Detection of HNC in the Interstellar Medium: Probing the Extreme Environment toward the Orion Hot Core. *Astrophys. J.* **2021**, *907*, 51.

(9) Huang, X.; Taylor, P. R.; Lee, T. J. Highly Accurate Quartic Force Field, Vibrational Frequencies, and Spectroscopic Constants for Cyclic and Linear $C_3H_3^+$. *J. Phys. Chem. A* **2011**, *115*, 5005–5016.

(10) Zhao, D.; Doney, K. D.; Linnartz, H. Laboratory Gas-Phase Detection of the Cyclopropenyl Cation (c-$C_3H_3^+$). *Astrophys. J. Lett.* **2014**, *791*, L28.

(11) Tennyson, J. Accurate Variational Calculations for Line Lists to Model the Vibration-Rotation Spectra of Hot Astrophysical Atmospheres. *Wiley Interdisciplinary Reviews: Computational Molecular Science* **2012**, *2*, 698–715.

(12) Huang, X.; Schwenke, D. W.; Lee, T. J. A Highly Accurate Potential Energy Surface and Initial IR Line List of $^{32}S^{16}O_2$ up to 8000 cm^{-1}. *J. Chem. Phys.* **2014**, *140*, 114311.

(13) Huang, X.; Schwenke, D. W.; Lee, T. J. Quantitative Validation of Ames IR Intensity and New Line Lists for $^{32/33/24}S^{18}O_2$, $^{32}S^{18}O_2$ and $^{16}O^{32}S^{18}O$. *J. Quant. Spectrosc. Radiat. Transfer* **2019**, *225*, 327–336.

(14) Li, H. Y.; Tennyson, J.; Yurchenko, S. N. ExoMol Line Lists – XXXII. The Rovibronic Spectrum of MgO. *Mon. Not. Royal Astron. Soc.* **2019**, *486*, 2351–2365.

(15) Fortenberry, R. C.; Huang, X.; Schwenke, D. W.; Lee, T. J. Limited Rotational and

Rovibrational Line Lists Computed with Highly Accurate Quartic Force Fields and *Ab Initio* Dipole Surfaces. *Spectrochim. Acta A* **2014**, *119*, 76–83.

(16) Cramer, C. J. *Essentials of Computational Chemistry: Theories and Models*, 2nd ed.; Wiley: West Sussex, England, 2004.

(17) Lee, T. J.; Martin, J. M. L.; Taylor, P. R. An Accurate *ab Initio* Quartic Force Field and Vibrational Frequencies for CH_4 and Its Isotopomers. *J. Chem. Phys.* **1995**, *102*, 254–261.

(18) Fortenberry, R. C.; Huang, X.; Yachmenev, A.; Thiel, W.; Lee, T. J. On the Use of Quartic Force Fields in Variational Calculations. *Chem. Phys. Lett.* **2013**, *574*, 1–12.

(19) Allen, W. D.; coworkers, 2005; *INTDER* 2005 is a General Program Written by W. D. Allen and Coworkers, which Performs Vibrational Analysis and Higher-Order Non-Linear Transformations.

(20) Barone, V.; Biczysko, M.; Puzzarini, C. Quantum Chemistry Meets Spectroscopy for Astrochemistry: Increasing Complexity toward Prebiotic Molecules. *Acc. Chem. Res.* **2015**, *48*, 1413–1422.

(21) Puzzarini, C.; Barone, V. Diving for Accurate Structures in the Ocean of Molecular Systems with the Help of Spectroscopy and Quantum Chemistry. *Acc. Chem. Res.* **2018**, *51*, 548–556.

(22) Fortenberry, R. C.; Lee, T. J. Computational Vibrational Spectroscopy for the Detection of Molecules in Space. *Ann. Rep. Comput. Chem.* **2019**, *15*, 173–202.

(23) Puzzarini, C.; Barone, V. The Challenging Playground of Astrochemistry: An Integrated Rotational Spectroscopy–Quantum Chemistry Strategy. *Phys. Chem. Chem. Phys.* **2020**, *22*, 6507–6523.

(24) Watson, J. K. G. In *Vibrational Spectra and Structure*; During, J. R., Ed.; Elsevier: Amsterdam, 1977; pp 1–89.

(25) Gaw, J. F.; Willets, A.; Green, W. H.; Handy, N. C. In *Advances in Molecular Vibrations and Collision Dynamics*; Bowman, J. M., Ratner, M. A., Eds.; JAI Press, Inc.: Greenwich, Connecticut, 1991; pp 170–185.

(26) Watson, J. K. G. Simplification of the Molecular Vibration-Rotation Hamiltonian. *Mol. Phys.* **1968**, *15*, 479–490.

(27) Franke, P. R.; Stanton, J. F.; Douberly, G. E. How to VPT2: Accurate and Intuitive Simulations of CH Stretching Infrared Spectra Using VPT2+K with Large Effective Hamiltonian Resonance Treatments. *J. Phys. Chem. A* **2021**, *125*, 1301–1324.

(28) Szabo, A.; Ostlund, N. S. *Modern Quantum Chemistry: Introduction to Advanced Electronic Structure Theory*; Dover: Mineola, NY, 1996.

(29) Møller, C.; Plesset, M. S. Note on an Approximation Treatment for Many-Electron Systems. *Phys. Rev.* **1934**, *46*, 618–622.

(30) Carter, S.; Bowman, J. M.; Handy, N. C. Extensions and Tests of "Multimodes": a Code to Obtain Accurate Vibration/Rotation Energies of Many-Mode Molecules. *Theor. Chem. Acc.* **1998**, *100*, 191–198.

(31) Bowman, J. M.; Carter, S.; Huang, X. MULTIMODE: a Code to Calculate Rovibrational Energies of Polyatomic Molecules. *Int. Rev. Phys. Chem.* **2003**, *22*, 533–549.

(32) Dateo, C. E.; Lee, T. J.; Schwenke, D. W. An Accurate Quartic Force-Field and Vibrational Frequencies for HNO and DNO. *J. Chem. Phys.* **1994**, *101*, 5853–5859.

(33) Carter, S.; Bowman, J. M. Variational Calculations of Rotational-Vibrational Energies of CH_4 and Isotopomers Using an Adjusted ab Initio Potential. *J. Phys. Chem. A* **2000**, *104*, 2355–2361.

(34) Morgan, W. J.; Fortenberry, R. C.; Schaefer III, H. F.; Lee, T. J. Vibrational Analysis of the Ubiquitous Interstellar Molecule Cyclopropenylidene (c-C_3H_2): The Importance of Numerical Stability. *Mol. Phys.* **2019**, *118*, e1589007.

(35) Helgaker, T.; Ruden, T. A.; Jørgensen, P.; Olsen, J.; Klopper, W. *A Priori* Calculation of Molecular Properties to Chemical Accuracy. *J. Phys. Org. Chem.* **2004**, *17*, 913–933.

(36) Raghavachari, K.; Trucks, G. W.; Pople, J. A.; Head-Gordon, M. A Fifth-Order Perturbation Comparison of Electron Correlation Theories. *Chem. Phys. Lett.* **1989**, *157*, 479–483.

(37) Dunning, T. H. Gaussian Basis Sets for Use in Correlated Molecular Calculations. I. The Atoms Boron through Neon and Hydrogen. *J. Chem. Phys.* **1989**, *90*, 1007–1023.

(38) Kendall, R. A.; Dunning, T. H.; Harrison, R. J. Electron Affinities of the First-Row Atoms Revisited. Systematic Basis Sets and Wave Functions. *J. Chem. Phys.* **1992**, *96*, 6796–6806.

(39) Lee, T. J.; Scuseria, G. E. The Vibrational Frequencies of Ozone. *J. Chem. Phys.* **1990**, *93*, 489–494.

(40) Lee, T. J.; Huang, X.; Dateo, C. E. The Effect of Approximating Some Molecular Integrals in Coupled-Cluster Calculations: Fundamental Frequencies and Rovibrational Spectroscopic Constants for isotopologues of Cyclopropenylidene. *Mol. Phys.* **2009**, *107*, 1139–1152.

(41) Gardner, M. B.; Westbrook, B. R.; Fortenberry, R. C.; Lee, T. J. Highly-Accurate Quartic Force Fields for the Prediction of Anharmonic Rotational Constants and Fundamental Vibrational Frequencies. *Spectrochim. Acta A* **2021**, *248*, 119184.

(42) Huang, X.; Lee, T. J. A Procedure for Computing Accurate *Ab Initio* Quartic Force Fields: Application to HO_2^+ and H_2O. *J. Chem. Phys.* **2008**, *129*, 044312.

(43) Huang, X.; Lee, T. J. Accurate *Ab Initio* Quartic Force Fields for NH_2^- and CCH^- and Rovibrational Spectroscopic Constants for Their Isotopologs. *J. Chem. Phys.* **2009**, *131*, 104301.

(44) Fortenberry, R. C.; Francisco, J. S. On the Detectability of the $\tilde{X}^2A''$ HSS, HSO, and HOS Radicals in the Interstellar Medium. *Astrophys. J.* **2017**, *835*, 243.

(45) Fuente, A.; Goicoechea, J. R.; Pety, J.; Gal, R. L.; Martín-Doménech, R.; Gratier, P.; Guzmán, V.; Roueff, E.; Loison, J. C.; Caro, G. M. M. et al. First Detection of Interstellar S_2H. *Astrophys. J.* **2017**, *851*, L49.

(46) Heikkilä, A.; Johansson, L. E. B.; Olofsson, H. Molecular Abundance Variations in the Magellanic Clouds. *Astron. Astrophys.* **1999**, *344*, 817–847.

(47) Cheung, A. C.; Rank, D. M.; Townes, C. H.; Thornton, D. D.; Welch, W. J. Detection of Water in Interstellar Regions by Its Microwave Radiation. *Nature* **1969**, *221*, 626.

(48) Martin, J. M. L.; Lee, T. J. The Atomization Energy and Proton Affinity of NH_3. An *Ab Initio* Calibration Study. *Chem. Phys. Lett.* **1996**, *258*, 136–143.

(49) Douglas, M.; Kroll, N. M. Quantum Electrodynamical Corrections to the Fine Structure of Helium. *Ann. Phys.* **1974**, *82*, 89–155.

(50) Gdanitz, R. J.; Ahlrichs, R. The Averaged Coupled-Pair Functional (ACPF): A Size-Extensive Modification of MR CI(SD). *Chem. Phys. Lett.* **1988**, *143*, 413–420.

(51) McCarthy, M. C.; Gottlieb, C. A.; Gupta, H.; Thaddeus, P. Laboratory and Astronomical Identification of the Negative Molecular Ion C_6H^-. *Astrophys. J.* **2006**, *652*, L141–L144.

(52) Cernicharo, J.; Guèlin, M.; Agùndez, M.; Kawaguchi, K.; McCarthy, M.; Thaddeus, P. Astronomical Detection of C_4H^-, the Second Interstellar Anion. *Astron. Astrophys.* **2007**, *467*, L37–L40.

(53) Brünken, S.; Gupta, H.; Gottlieb, C. A.; McCarthy, M. C.; Thaddeus, P. Detection of the Carbon Chain Negative Ion C_8H^- in TMC-1. *Astrophys. J.* **2007**, *664*, L43–L46.

(54) Remijan, A. J.; Hollis, J. M.; Lovas, F. J.; Cordiner, M. A.; Millar, T. J.; Markwick-Kemper, A. J.; Jewell, P. R. Detection of C_8H^- and comparison with C_8H toward IRC+10216. *Astrophys. J.* **2007**, *664*, L47–L50.

(55) Fortenberry, R. C. Interstellar Anions: The Role of Quantum Chemistry. *J. Phys. Chem. A* **2015**, *119*, 9941–9953.

(56) van Dishoeck, E. F.; Jansen, D. J.; Schilke, P.; Phillips, T. G. Detection of the Interstellar NH_2 Radical. *Astrophys. J.* **1993**, *416*, L83–L86.

(57) Persson, C. M.; Hajigholi, M.; Hassel, G. E.; Olofsson, A. O. H.; Black, J. H.; Herbst, E.; Müller, H. S. P.; Cernicharo, J.; Wirström, E. S.; Olberg, M. et al. Upper Limits to Interstellar NH^+ and *para*-NH_2 Abundances. Herschel-HIFI Observations towards Sgr B2 (M) and G10.6-0.4 (W31C). *Astron. Astrophys.* **2014**, *567*, A130.

(58) Allamandola, L. J. In *PAHs and the Universe: A Symposium to Celebrate the 25th Anniversary of the PAH Hypothesis*; Joblin, C., Tielens, A. G. G. M., Eds.; EAS Publication Series: Cambridge, UK, 2011.

(59) Martin, J. M. L.; Taylor, P. R. Basis Set Convergence for Geometry and Harmonic Frequencies. Are *h* Functions Enough? *Chem. Phys. Lett.* **1994**, *225*, 473–479.

(60) Fortenberry, R. C.; Huang, X.; Francisco, J. S.; Crawford, T. D.; Lee, T. J. The *trans*-HOCO Radical: Fundamental Vibrational Frequencies, Quartic Force Fields, and Spectroscopic constants. *J. Chem. Phys.* **2011**, *135*, 134301.

(61) Francisco, J. S.; Muckerman, J. T.; Yu, H.-G. HOCO Radical Chemistry. *Acc. Chem. Res.* **2010**, *43*, 1519–1526.

(62) Yu, H.; Muckerman, J.; Francisco, J. Direct *ab initio* dynamics study of the OH plus HOCO reaction. *J. Phys. Chem. A* **2005**, *109*, 5230–5236.

(63) Yu, H.-G.; Muckerman, J. T.; Francisco, J. S. Quantum force molecular dynamics study of the reaction of O atoms with HOCO. *J. Chem. Phys.* **2007**, *127*, 094302.

(64) Sears, T. J.; Fawzy, W. M.; Johnson, P. M. Transient Diode-Laser Absorption-Spectroscopy of the ν_2 Fundamental of *trans*-HOCO and DOCO. *J. Chem. Phys.* **1992**, *97*, 3996–4007.

(65) Petty, J. T.; Moore, C. B. Transient Infrared-Absorption Spectrum of the ν_1 Fundamental of *trans*-HOCO. *J. Mol. Spectrosc.* **1993**, *161*, 149–156.

(66) Fortenberry, R. C.; Huang, X.; Francisco, J. S.; Crawford, T. D.; Lee, T. J. Vibrational Frequencies and Spectroscopic Constants from Quartic Force Fields for *cis*-HOCO: The Radical and the Anion. *J. Chem. Phys.* **2011**, *135*, 214303.

(67) Fortenberry, R. C. The Rovibrational Nature of *cis*- and *trans*-HNNS: A Possible Nitrogen Molecule Progenitor. *J. Chem. Phys.* **2016**, *145*, 204302.

(68) Fortenberry, R. C.; Huang, X.; Francisco, J. S.; Crawford, T. D.; Lee, T. J. Quartic Force Field Predictions of the Fundamental Vibrational Frequencies and Spectroscopic Constants of the Cations $HOCO^+$ and $DOCO^+$. *J. Chem. Phys.* **2012**, *136*, 234309.

(69) Fortenberry, R. C. Rovibrational Characterization of the Proton-Bound, Noble Gas Complexes: $ArHNe^+$, $ArHAr^+$, and $NeHNe^+$. *ACS Earth Space Chem.* **2017**, *1*, 60–69.

(70) Stephan, C. J.; Fortenberry, R. C. The Interstellar Formation and Spectra of the Noble Gas, Proton-Bound $HeHHe^+$, $HeHNe^+$ and $HeHAr^+$ Complexes. *Mon. Not. Royal Astron. Soc.* **2017**, *469*, 339–346.

(71) Fortenberry, R. C.; Huang, X.; Francisco, J. S.; Crawford, T. D.; Lee, T. J. Fundamental Vibrational Frequencies and Spectroscopic Constants of $HOCS^+$, $HSCO^+$, and Isotopologues via Quartic Force Fields. *J. Phys. Chem. A.* **2012**, *116*, 9582–9590.

(72) Fortenberry, R. C.; Francisco, J. S. Factors Affecting the Spectroscopic Observation of Bridged HPSi and Linear HSiP in Astrophysical/Interstellar Media. *Astrophys. J.* **2017**, *843*, 124.

(73) Fortenberry, R. C.; Crawford, T. D.; Lee, T. J. The Potential Interstellar Anion CH_2CN^-: Spectroscopic Constants, Vibrational Frequencies, and Other Considerations. *Astrophys. J.* **2013**, *762*, 121.

(74) Fortenberry, R. C.; Thackston, R.; Francisco, J. S.; Lee, T. J. Toward the Laboratory Identification of the Not-So-Simple NS_2 Neutral and Anion Isomers. *J. Chem. Phys.* **2017**, *147*, 074303.

(75) Huang, X.; Fortenberry, R. C.; Lee, T. J. Spectroscopic Constants and Vibrational Frequencies for *l*-C_3H^+ and Isotopologues from Highly-Accurate Quartic Force Fields: The Detection of *l*-C_3H^+ in the Horsehead Nebula PDR Questioned. *Astrophys. J. Lett.* **2013**, *768*, 25.

(76) Brünken, S.; Kluge, L.; Stoffels, A.; Asvany, O.; Schlemmer, S. Laboratory Rotational Spectrum of *l*-C_3H^+ and Confirmation of Its Astronomical Detection. *Astrophys. J.* **2014**, *783*, L4.

(77) Fortenberry, R. C.; Lee, T. J.; Huang, X. Towards Completing the Cyclopropanylidene Cycle: Rovibrational Analysis of Cyclic N_3^+, CNN, $HCNN^+$, and CNC^-. *Phys. Chem. Chem. Phys.* **2017**, *19*, 22860–22869.

(78) Fortenberry, R. C.; Huang, X.; Crawford, T. D.; Lee, T. J. High-Accuracy Quartic Force Field Calculations for the Spectroscopic Constants and Vibrational Frequencies

of $1^1A'$ l-C_3H^-: A Possible Link to Lines Observed in the Horsehead Nebula PDR. *Astrophys. J.* **2013**, *772*, 39.

(79) Fortenberry, R. C.; Francisco, J. S.; Lee, T. J. Quantum Chemical Rovibrational Analysis of the HOSO Radical. *J. Phys. Chem. A* **2017**, *121*, 8108–8114.

(80) Huang, X.; Fortenberry, R. C.; Lee, T. J. Protonated Nitrous Oxide, $NNOH^+$: Fundamental Vibrational Frequencies and Spectroscopic Constants from Quartic Force Fields. *J. Chem. Phys.* **2013**, *139*, 084313.

(81) Thackston, R.; Fortenberry, R. C. Quantum Chemical Spectral Characterization of $CH_2NH_2^+$ for Remote Sensing of Titan's Atmosphere. *Icarus* **2018**, *299*, 187–193.

(82) Fortenberry, R. C.; Huang, X.; McCarthy, M. C.; Crawford, T. D.; Lee, T. J. Fundamental Vibrational Frequencies and Spectroscopic Constants of *cis*- and *trans*-HOCS, HSCO, and Isotopologues via Quartic Force Fields. *J. Phys. Chem. B* **2014**, *118*, 6498–6510.

(83) Kloska, K. A.; Fortenberry, R. C. Gas-Phase Spectra of MgO Molecules: A Possible Connection from Gas-Phase Molecules to Planet Formation. *Mon. Not. Royal Astron. Soc.* **2018**, *474*, 2055–2063.

(84) Bassett, M. K.; Fortenberry, R. C. Magnesium in the Formaldehyde: The Theoretical Rovibrational Analysis of $\tilde{X}\ ^3B_1$ $MgCH_2$. *J. Molec. Spectrosc.* **2018**, *344*, 61–64.

(85) Palmer, C. Z.; Fortenberry, R. C. Rovibrational Considerations for the Monomers and Dimers of Magnesium Hydride (MgH_2) and Magnesium Fluoride (MgF_2). *J. Phys. Chem. A* **2018**, *122*, 7079–7088.

(86) Fortenberry, R. C.; Huang, X.; Crawford, T. D.; Lee, T. J. Quartic Force Field Rovibrational Analysis of Protonated Acetylene, $C_2H_3^+$, and Its Isotopologues. *J. Phys. Chem. A* **2014**, *118*, 7034–7043.

(87) Fortenberry, R. C.; Francisco, J. S. A Possible Progenitor of the Interstellar Sulfide Bond: Rovibrational Characterization of the Hydrogen Disulfide Cation $HSSH^+$. *Astrophys. J.* **2018**, *856*, 30.

(88) Fortenberry, R. C.; Trabelsi, T.; Francisco, J. S. Hydrogen Sulfide as a Scavenger of Sulfur Atomic Cation. *J. Phys. Chem. A* **2018**, *122*, 4983–4987.

(89) Fortenberry, R. C.; Huang, X.; Crawford, T. D.; Lee, T. J. Quantum Chemical Rovibrational Data for the Interstellar Detection of *c*-C_3H^-. *Astrophys. J.* **2014**, *796*, 139.

(90) Fortenberry, R. C.; Novak, C. M.; Lee, T. J. Rovibrational Analysis of *c*-SiC_2H_2: Further Evidence for Out-of-Plane Bending Issues in Correlated Methods. *J. Chem. Phys.* **2018**, *149*, 024303.

(91) Theis, R. A.; Morgan, W. J.; Fortenberry, R. C. ArH_2^+ and NeH_2^+ as Global Minima in the $Ar^+/Ne^+ + H_2$ Reactions: Energetic, Spectroscopic, and Structural Data. *Mon. Not. R. Astron. Soc.* **2015**, *446*, 195–204.

(92) Morgan, W. J.; Huang, X.; Schaefer III, H. F.; Lee, T. J. Astrophysical Sulfur in Diffuse and Dark Clouds: The Fundamental Vibrational Frequencies and Spectroscopic Constants of Hydrogen Sulfide Cation (H_2S^+). *Mon. Not. Royal Astron. Soc.* **2018**, *480*, 3483–3490.

(93) Theis, R. A.; Fortenberry, R. C. Trihydrogen Cation with Neon and Argon: Structural, Energetic, and Spectroscopic Data from Quartic Force Fields. *J. Phys. Chem. A* **2015**, *119*, 4915–4922.

(94) McDonald II, D. C.; Rittgers, B.; Theis, R. A.; Fortenberry, R. C.; Marks, J. H.; Leicht, D.; Duncan, M. A. nfrared Spectroscopy and Anharmonic Theory of $H_3{}^+Ar_{2,3}$ Complexes: The Role of Symmetry in Solvation. *J. Chem. Phys.* **2020**, *153*, 134305.

(95) Fortenberry, R. C.; Ascenzi, D. $ArCH_2^+$: A Detectable Noble Gas Molecule. *Chem. Phys. Chem.* **2018**, *19*, 1–6.

(96) Fortenberry, R. C. The $ArNH_2^+$ Noble Gas Molecule: Stability, Vibrational Frequencies, and Spectroscopic Constants. *J. Molec. Spectrosc.* **2019**, *357*, 4–8.

(97) Fortenberry, R. C.; Lee, T. J. Rovibrational and Energetic Analysis of the Hydroxyethynyl Anion ($CCOH^-$). *Mol. Phys.* **2015**, *113*, 2012–2017.

(98) Fortenberry, R. C.; Lee, T. J.; Inostroza-Pino, N. The Possibility of $:CNH_2^+$ within Titan's Atmosphere: Rovibrational Analysis T of $:CNH_2^+$ and $:CCH_2$. *Icarus* **2019**, *321*, 260–265.

(99) Fortenberry, R. C.; Yu, Q.; Mancini, J. S.; Bowman, J. M.; Lee, T. J.; Crawford, T. D.; Klemperer, W. F.; Francisco, J. S. Communication: Spectroscopic Consequences of Proton Delocalization in $OCHCO^+$. *J. Chem. Phys.* **2015**, *143*, 071102.

(100) Yu, Q.; Bowman, J. M.; Fortenberry, R. C.; Mancini, J. S.; Lee, T. J.; Crawford, T. D.; Klemperer, W.; Francisco, J. S. The Structure, Anharmonic Vibrational Frequencies, and Intensities of $NNHNN^+$. *J. Phys. Chem. A* **2015**, *119*, 11623–11631.

(101) Fortenberry, R. C.; Lee, T. J.; Francisco, J. S. Towards the Astronomical Detection of the Proton-Bound Complex NN-HCO^+: Implications for the Spectra of Protoplanetary Disks. *Astrophys. J.* **2016**, *819*, 141.

(102) Fortenberry, R. C.; Lee, T. J.; Francisco, J. S. Quantum Chemical Analysis of the $CO{-}HNN^+$ Proton-Bound Complex. *J. Phys. Chem. A* **2016**, *120*, 7745–7752.

(103) Del Rio, W. A.; Fortenberry, R. C. Rotational and Vibrational Fingerprints of the Oxywater Cation (H_2OO^+), a Possible Precursor to Abiotic O_2. *J. Molec. Spectrosc.* **2019**, *364*, 111183.

(104) Fortenberry, R. C.; Francisco, J. S. Quartic Force Field-derived Vibrational Frequencies and Spectroscopic Constants for the Isomeric Pair SNO and OSN and Isotopologues. *J. Chem. Phys.* **2015**, *143*, 084308.

(105) Fortenberry, R. C.; Francisco, J. S. Energetics, Structure, and Rovibrational Spectroscopic Properties of the Sulfurous Anions SNO^- and OSN^-. *J. Chem. Phys.* **2015**, *143*, 184301.

(106) Dubois, D.; Sciamma-O'Brien, E.; Fortenberry, R. C. The Fundamental Vibrational Frequencies and Spectroscopic Constants of the Dicyanoamine Anion, $NCNCN^-$ ($C_2N_3^-$): Quantum Chemical Analysis for Astrophysical and Planetary Environments. *Astrophys. J.* **2019**, *883*, 109.

(107) Fortenberry, R. C.; Lukemire, J. A. Electronic and Rovibrational Quantum Chemical Analysis of C_3P^-: The Next Interstellar Anion? *Mon. Not. R. Astron. Soc.* **2015**, *453*, 2824–2829.

(108) Trabelsi, T.; Davis, M. C.; Fortenberry, R. C.; Francisco, J. S. Spectroscopic Investigation of [Al,N,C,O] Refractory Molecules. *J. Chem. Phys.* **2019**, *151*, 244303.

(109) Fortenberry, R. C.; Thackston, R. Optimal Cloud Use of Quartic Force Fields: The First Purely Commercial Cloud Computing Based Study for Rovibrational Analysis of $SiCH^-$. *Int. J. Quant. Chem.* **2015**, *115*, 1650–1657.

(110) Bera, P. P.; Huang, X.; Lee, T. J. Highly Accurate Quartic Force Field and Rovibrational Spectroscopic Constants for the Azirinyl Cation (c-$C_2NH_2^+$) and Its Isomers. *J. Phys. Chem. A* **2020**, *124*, 362–370.

(111) Theis, R. A.; Fortenberry, R. C. Potential Interstellar Noble Gas Molecules: $ArOH^+$ and $NeOH^+$ Rovibrational Analysis from Quantum Chemical Quartic Force Fields. *Molec. Astrophys.* **2016**, *2*, 18–24.

(112) Novak, C. M.; Fortenberry, R. C. Theoretical Rovibrational Analysis of the Covalent Noble Gas Compound $ArNH^+$. *J. Molec. Spectrosc.* **2016**, *322*, 29–32.

(113) Novak, C. M.; Fortenberry, R. C. The Rovibrational Spectra of Three, Stable Noble Gas Molecules: $NeCCH^+$, $ArCCH^+$, and $ArCN^+$. *Phys. Chem. Chem. Phys.* **2017**, *19*, 5230–5238.

(114) Fortenberry, R. C.; Gwaltney, S. R. $NeON^+$: An Atom *AND* a Molecule. *ACS Earth Space Chem.* **2018**, *2*, 491–495.

(115) Fortenberry, R. C.; Trabelsi, T.; Francisco, J. S. Anharmonic Frequencies and Spectroscopic Constants of OAlOH and AlOH: Strong Bonding but Unhindered Motion. *J. Phys. Chem. A* **2020**, *124*, 8834–8841.

(116) Fortenberry, R. C.; Trabelsi, T.; Francisco, J. S. Theoretical Rovibrational Characterization of HAlNP: Weak Bonding but Strong Intensities. *J. Molec. Spectrosc.* **2020**, *377*, 111422.

(117) Kitchens, M. J. R.; Fortenberry, R. C. The Rovibrational Nature of Closed-Shell Third-Row Triatomics: HOX and HXO, X = Si^+, P, S^+, and Cl. *Chem. Phys.* **2016**, *472*, 119–127.

(118) Dallas, J. D.; Westbrook, B. R.; Fortenberry, R. C. Anharmonic Vibrational Frequencies and Spectroscopic Constants for the Detection of Ethynol in Space. *Frontiers Astron. Space Sci.* **2021**, *7*, 626407.

(119) Finney, B.; Fortenberry, R. C.; Francisco, J. S.; Peterson, K. A. A Spectroscopic Case for SPSi Detection: The Third-Row in a Single Molecule. *J. Chem. Phys.* **2016**, *145*, 124311.

(120) Fortenberry, R. C.; Francisco, J. S. Anharmonic Fundamental Vibrational Frequencies

and Spectroscopic Constants of the Potential HSO_2 Radical Astromolecule. *J. Chem. Phys.* **2021**, *155*, 114301.

(121) Minh, Y. C.; Irvine, W. M.; Ziurys, L. M. Observations of interstellar $HOCO^+$: Abundance enhancements towards the galactic center. *Astrophys. J.* **1988**, *334*, 175–181.

(122) Minh, Y. C.; Brewer, M. K.; Irvine, W. M.; Friberg, P.; Johansson, L. E. B. Abundance and chemistry of interstellar $HOCO^+$. *Astron. Astrophys.* **1991**, *244*, 470–476.

(123) Pety, J.; Gratier, P.; Guzmán, V.; Roueff, E.; Gerin, M.; Goicoechea, J. R.; Bardeau, S.; Sievers, A.; Petit, F. L.; Bourlot, J. L. et al. The IRAM-30 m Line Survey of the Horsehead PDR II. First Detection of the *l*-C_3H^+ Hydrocarbon Cation. *Astron. Astrophys.* **2012**, *548*, A68.

(124) Barlow, M. J.; Swinyard, B. M.; Owen, P. J.; Cernicharo, J.; Gomez, H. L.; Ivison, R. J.; Krause, O.; Lim, T. L.; Matsuura, M.; Miller, S. et al. Detection of a Noble Gas Molecular Ion, $^{36}ArH^+$, in the Crab Nebula. *Science* **2013**, *342*, 1343–1345.

(125) Wagner, J. P.; McDonald II, D. C.; Duncan, M. A. An Argon–Oxygen Covalent Bond in the $ArOH^+$ Molecular Ion. *Angew. Chem. Int. Ed* **2018**, *57*, 5081–5085.

(126) Wagner, J. P.; Giles, S. M.; Duncan, M. A. Gas Phase Infrared Spectroscopy of the $H_2C{=}NH_2^+$ Methaniminium Cation. *Chem. Phys. Lett.* **2019**, *726*, 53–56.

(127) Thackston, R.; Fortenberry, R. C. The Performance of Low-Cost Commercial Cloud Computing as an Alternative in Computational Chemistry. *J. Comput. Chem.* **2015**, *36*, 926–933.

(128) Lee, T. J.; Schaefer III, H. F. The Classical and Nonclassical Forms of Protonated Acetylene, $C_2H_3^+$: Structures, Vibrational Frequencies, and Infrared Intensities from Explicitly Correlated Wave Functions. *J. Chem. Phys.* **1986**, *85*, 3437–3443.

(129) Adler, T. B.; Knizia, G.; Werner, H.-J. A Simple and Efficient CCSD(T)-F12 Approximation. *J. Chem. Phys.* **2007**, *127*, 221106.

(130) Knizia, G.; Adler, T. B.; Werner, H.-J. Simplified CCSD(T)-F12 Methods: Theory and Benchmarks. *J. Chem. Phys.* **2009**, *130*, 054104.

(131) Huang, X.; Valeev, E. F.; Lee, T. J. Comparison of One-Particle Basis Set Extrapolation to Explicitly Correlated Methods for the Calculation of Accurate Quartic Force Fields, Vibrational Frequencies, and Spectroscopic Constants: Application to H_2O, N_2H^+, $NO_2{}^+$, and C_2H_2. *J. Chem. Phys.* **2010**, *133*, 244108.

(132) Fortenberry, R. C.; Lee, T. J.; Layfield, J. P. Communication: The Failure of Correlation to Describe Carbon=Carbon Bonding in Out-of-Plane Bends. *J. Chem. Phys.* **2017**, *147*, 221101.

(133) Fortenberry, R. C.; Novak, C. M.; Layfield, J. P.; Matito, E.; Lee, T. J. Overcoming the Failure of Correlation for Out-of-Plane Motions in a Simple Aromatic: Rovibrational Quantum Chemical Analysis of *c*-C_3H_2. *J. Chem. Theor. Comput.* **2018**, *14*, 2155–2164.

(134) Lee, T. J.; Fortenberry, R. C. The Unsolved Issue with Out-of-Plane Bending Frequencies for C=C Multiply Bonded Systems. *Spectrochim. Acta A* **2021**, *248*, 119148.

(135) Agbaglo, D.; Fortenberry, R. C. The Performance of CCSD(T)-F12/aug-cc-pVTZ for the Computation of Anharmonic Fundamental Vibrational Frequencies. *Int. J. Quantum Chem.* **2019**, *119*, e25899.

(136) Agbaglo, D.; Fortenberry, R. C. The Performance of Explicitly Correlated Wavefunctions [CCSD(T)-F12b] in the Computation of Anharmonic Vibrational Frequencies. *Chem. Phys. Lett.* **2019**, *734*, 136720.

(137) Agbaglo, D.; Lee, T. J.; Thackston, R.; Fortenberry, R. C. A Small Molecule with PAH Vibrational Properties and a Detectable Rotational Spectrum: *c*-(C)C_3H_2, Cyclopropenylidenyl Carbene. *Astrophys. J.* **2019**, *871*, 236.

(138) Agbaglo, D.; Fortenberry, R. C. uantum Chemical Rovibrational Characterization of CH_2ClH^+, a Low-Energy Isomer of Ionized Chloromethane. *ACS Earth Space Chem.* **2019**, *3*, 1296–1301.

(139) Fortenberry, R. C.; Peters, D.; Ferari, B. C.; Bennett, C. J. Rovibrational Spectral Analysis of CO_3 and C_2O_3: Potential Sources for O_2 Observed in Comet 67P/Churyumov-Gerasimenko. *Astrophys. J. Lett.* **2019**, *886*, L10.

(140) Valencia, E. M.; Worth, C. J.; Fortenberry, R. C. Enstatite ($MgSiO_3$) and Forsterite (Mg_2SiO_4) Monomers and Dimers: Highly-Detectable Infrared and Radioastronomical Molecular Building Blocks. *Mon. Not. Royal Astron. Soc.* **2020**, *492*, 276–282.

(141) Westbrook, B. R.; Rio, W. A. D.; Lee, T. J.; Fortenberry, R. C. Overcoming the Out-of-Plane Bending Issue in an Aromatic Hydrocarbon: The Anharmonic Vibrational Frequencies of *c*-(CH)$C_3H_2^+$. *Phys. Chem. Chem. Phys.* **2020**, *22*, 12951–12958.

(142) Inostroza-Pino, N.; Palmer, C. Z.; Lee, T. J.; Fortenberry, R. C. Theoretical Rovibrational Characterization of the *cis/trans*-HCSH and H_2SC Isomers of the Known Interstellar Molecule Thioformaldehyde. *J. Molec. Spectrosc.* **2020**, *369*, 111273.

(143) Gardner, M. B.; Westbrook, B. R.; Fortenberry, R. C. Anharmonic Vibrational Frequencies for Small Clusters of Silicon and Oxygen: SiO_2, SiO_3, Si_2O_3, & Si_2O_4. *Planet Space Sci.* **2020**, *193*, 105176.

(144) Westbrook, B. R.; Valencia, E. M.; Rushing, S. C.; Tschumper, G. S.; Fortenberry, R. C. Anharmonic Vibrational Frequencies of Ammonia Borane (BH_3NH_3). *J. Chem. Phys* **2021**, *154*, 041104.

(145) Watrous, A. G.; Davis, M. C.; Fortenberry, R. C. Pathways to Detection of Strongly-Bound Inorganic Species: The Vibrational and Rotational Spectral Data of AlH_2OH, HMgOH, AlH_2NH_2, and $HMgNH_2$. *Frontiers in Astronomy and Space Sciences* **2021**, *8*, 17.

(146) Watrous, A. G.; Westrbook, B. R.; Davis, M. C.; Fortenberry, R. C. Vibrational and Rotational Spectral Data for Possible Interstellar Detection of AlH_3OH_2, SiH_3OH, and SiH_3NH_2. *Mon. Not. Royal Astron. Soc.* **2021**, *accepted*.

(147) Westbrook, B. R.; Fortenberry, R. C. Anharmonic Frequencies of $(MO)_2$ & Related Hydrides for M = Mg, Al, Si, P, S, Ca, & Ti and Heuristics for Predicting Anharmonic Corrections of Inorganic Oxides. *J. Phys. Chem. A* **2020**, *124*, 3191–3204.

(148) Cernicharo, J.; Guèlin, M.; Agundez, M.; McCarthy, M. C.; Thaddeus, P. Detection of C_5N^- and Vibrationally Excited C_6H in IRC+10216. *Astrophys. J.* **2008**, *688*, L83–L86.

(149) Turner, B. E. Detection of Vibrationally Excited SiS in IRC+10216. *Astron. Astrophys.* **1987**, *183*, L23–L26.

(150) Lacy, J. H.; Evans II, N. J.; Achtermann, J. M.; Bruce, D. E.; Arens, J. F.; Carr, J. S. Discovery of Interstellar Acetylene. *Astrophys. J.* **1989**, *342*, L43–L46.

(151) d'Hendecourt, L. B.; Jourdain de Muizon, M. The Discovery of Interstellar Carbon Dioxide. *Astron. Astrophys.* **1989**, *223*, L5–L8.

(152) Cami, J.; Bernard-Salas, J.; Peeters, E.; Malek, S. E. Detection of C_{60} and C_{70} in Young Planetary Nebulea. *Science* **2010**, *329*, 1180–1192.

(153) McGuire, B. A. 2018 Census of Interstellar, Circumstellar, Extragalactic, Protoplanetary Disk, and Exoplanetary Molecules. *Astrophys. J. Suppl. Ser.* **2018**, *239*, 17.

(154) Mills, I. M. In *Molecular Spectroscopy - Modern Research*; Rao, K. N., Mathews, C. W., Eds.; Academic Press: New York, 1972; pp 115–140.

(155) Papousek, D.; Aliev, M. R. *Molecular Vibration-Rotation Spectra*; Elsevier: Amsterdam, 1982.

(156) Thaddeus, P.; Cummins, S. E.; Linke, R. A. Identification of the SiCC Radical toward IRC +10216: The First Molecular Ring in an Astronomical Source. *Astrophys. J.* **1984**, *283*, L45–L48.

(157) Cernicharo, J.; McCarthy, M. C.; Gottlieb, C. A.; Agúndez, M.; Prieto, L. V.; Baraban, J. H.; Changala, P. B.; Guéédin, M.; Kahane, C.; Martin-Drumel, M. A. et al. Discovery of SiCSi in IRC+10216: A Missing Link between Gas and Dust Carriers of Si-C Bonds. *Astrophys. J. Lett.* **2015**, *806*, L3.

(158) Fortenberry, R. C.; Lee, T. J.; Müller, H. S. P. Excited Vibrational Level Rotational Constants for SiC_2: A Sensitive Molecular Diagnostic for Astrophysical Conditions. *Molec. Astrophys.* **2015**, *1*, 13–19.

(159) Butenhoff, T. J.; Rohlfing, E. A. Laser-Induced Fluorescence Spectroscopy of Jet-Cooled SiC_2. *J. Chem. Phys.* **1991**, *95*, 1–8.

(160) Campbell, E. K.; Holz, M.; Gerlich, D.; Maier, J. P. Laboratory confirmation of C_{60}^+ as the carrier of two diffuse interstellar bands. *Nature* **2015**, *523*, 322–324.

(161) Cordinder, M. A.; Linnartz, H.; Cox, N. L. J.; Cami, J.; Najarro, F.; Proffitt, C. R.; Lallement, R.; Ehrenfreund, P.; Foing, B. H.; Gull, T. R. et al. Confirming Interstellar C_{60}^+ Using the *Hubble Space Telescope*. *Astrophys. J. Lett.* **2019**, *875*, L28.

(162) Heger, M. L. The spectra of certain class B stars in the regions 5630Å-6680Åand 3280Å-3380Å. *Lick Observatory Bulletin* **1922**, *10*, 146.

(163) Merrill, P. W. Unidentified Interstellar Lines. *Publ. Astron. Soc. Pacific* **1934**, *46*, 206–207.

(164) Merrill, P. W. Stationary Lines in the Spectrum of the Binary Star Boss 6142. *Astrophys. J.* **1936**, *83*, 126–128.

(165) McKellar, A. Evidence for the Molecular Origin of Some Hitherto Unidentified Interstellar Lines. *Publ. Astron. Soc. Pac.* **1940**, *52*, 187–192.

(166) Douglas, A. E. Origin of Diffuse Interstellar Lines. *Nature.* **1977**, *269*, 130–132.

(167) Sarre, P. J. The Diffuse Interstellar Bands: A Major Problem in Astronomical Spectroscopy. *J. Mol. Spectrosc.* **2006**, *238*, 1–10.

(168) McCall, B. J.; Griffin, R. E. On the Discovery of the Diffuse Interstellar Bands. *Proc. Royal Soc. A* **2013**, *469*, 20120604.

(169) Swings, P.; Rosenfield, L. Considerations Regarding Interstellar Molecules. *Astrophys. J.* **1937**, *86*, 483–486.

(170) Adams, W. S. Some Results with the COUDÉ Spectrograph of the Mount Wilson Observatory. *Astrophys. J.* **1941**, *93*, 11–23.

(171) Douglas, A. E.; Herzberg, G. Note on CH^+ in Interstellar Space and in the Laboratory. *Astrophys. J.* **1941**, *94*, 381.

(172) Huggins, W. Preliminary Note on the Photographic Spectrum of Comet b 1881. *Proceedings of the the Royal Society of London* **1881**, *33*, 1–3.

(173) Fowler, A. Investigations Relating to the Spectra of Comets. *Mon. Not. Royal Astron. Soc.* **1910**, *70*, 484–496.

(174) Swings, P.; Page, T. The Spectrum of Comet Bester (1947k). *Astrophys. J.* **1950**, *111*, 530–554.

(175) Herzberg, G.; Lew, H. Tentative Identffication of the H_2O^+ Ion in Comet Kohoutek. *Astron. Astrophys.* **1974**, *31*, 123–124.

(176) Pierce, D. M.; A'Hearn, M. F. An Analysis of CO Production in Cometary Comae: Contributions from Gas-Phase Phenomena. *Astrophys. J.* **2010**, *718*, 340–347.

(177) Fortenberry, R. C.; Pierce, D. M.; Bodewits, D. Knowledge Gaps in the Emission Spectra of Oxygen-Bearing Molecular Cations. *Astrophys. J. Suppl. Ser.* **2021**, *256*, 6.

(178) Fortenberry, R. C.; Huang, X.; Crawford, T. D.; Lee, T. J. The 1 $^3A'$ HCN and 1 $^3A'$ HCO^+ Vibrational Frequencies and Spectroscopic Constants from Quartic Force Fields. *J. Phys. Chem. A.* **2013**, *117*, 9324–9330.

(179) Fortenberry, R. C.; Crawford, T. D.; Lee, T. J. Vibrational Frequencies and Spectroscopic Constants for 1 $^3A'$ HNC and 1 $^3A'$ HOC^+ from High-Accuracy Quartic Force Fields. *J. Phys. Chem. A.* **2013**, *117*, 11339–11345.

(180) Inostroza, N.; Huang, X.; Lee, T. J. Accurate *ab initio* Quartic Force Fields of Cyclic and Bent HC_2N Isomers. *J. Chem. Phys.* **2011**, *135*, 244310.

(181) Czekner, J.; Cheung, L. F.; Johnson, E. L.; Fortenberry, R. C.; Wang, L.-S. A High Resolution Photoelectron Imaging and Theoretical Study of CP^- and C_2P^-. *J. Chem. Phys.* **2018**, *148*, 044301.

(182) Morgan, W. J.; Fortenberry, R. C. Additional Diffuse Functions in Basis Sets for Dipole-Bound Excited States of Anions. *Theor. Chem. Acc.* **2015**, *134*, 47.

(183) Stanton, J. F.; Bartlett, R. J. The Equation of Motion Coupled-Cluster Method - A Systematic Biorthogonal Approach to Molecular Excitation Energies, Transition-Probabilities, and Excited-State Properties. *J. Chem. Phys.* **1993**, *98*, 7029–7039.

(184) Krylov, A. I. Equation-of-Motion Coupled Cluster Methods for Open-Shell and Electronically Excited Species: The Hitchiker's Guide to Fock Space. *Ann. Rev. Phys. Chem.* **2007**, *59*, 433–463.

(185) Fortenberry, R. C.; King, R. A.; Stanton, J. F.; Crawford, T. D. A Benchmark Study of the Vertical Electronic Spectra of the Linear Chain Radicals C_2H and C_4H. *J. Chem. Phys.* **2010**, *132*, 144303.

(186) Christiansen, O.; Koch, H.; Jørgensen, P. Response functions in the CC3 iterative triple excitation model. *J. Chem. Phys.* **1995**, *103*, 7429–7441.

(187) Koch, H.; Christiansen, O.; Jørgensen, P.; de Meràs, A. M. S.; Helgaker, T. The CC3 Model: An Iterative Coupled Cluster Approach including Connected Triples. *J. Chem. Phys.* **1997**, *106*, 1808–1818.

(188) Smith, C. E.; King, R. A.; Crawford, T. D. Coupled Cluster Excited Methods Including Triple Excitations for Excited States of Radicals. *J. Chem. Phys.* **2005**, *122*, 054110–1–8.

(189) Morgan, W. J.; Fortenberry, R. C. Quartic Force Fields for Excited Electronic States: Rovibronic Reference Data for the 1 $^2A'$ and 1 $^2A''$ States of the Isoformyl Radical, HOC. *Spectrochim. Acta A* **2015**, *135*, 965–972.

(190) Morgan, W. J.; Fortenberry, R. C. Theoretical Rovibronic Treatment of the $\widetilde{X}$ $^2\Sigma^+$ and $\widetilde{A}$ $^2\Pi$ States of C_2H & $\widetilde{X}$ $^1\Sigma^+$ State of C_2H^- from Quartic Force Fields. *J. Phys. Chem. A* **2015**, *119*, 7013–7025.

(191) Bassett, M. K.; Fortenberry, R. C. Symmetry Breaking and Spectral Considerations of the Surprisingly Floppy *c*-C_3H Radical and the Related Dipole-Bound Excited State of *c*-C_3H^-. *J. Chem. Phys.* **2017**, *146*, 224303.

(192) Davis, M. C.; Fortenberry, R. C. (T)+EOM Quartic Force Fields for Theoretical Vibrational Spectroscopy of Electronically Excited States. *J. Chem. Theor. Comput.* **2021**, *17*, 4374–4382.

(193) McGuire, B. A.; Burkhardt, A. M.; Kalenskii, S.; Shingledecker, C. N.; Remijan, A. J.; Herbst, E.; McCarthy, M. C. Detection of the Aromatic Molecule Benzonitrile (*c*-C_6H_5CN) in the Interstellar Medium. *Science* **2018**, *359*, 202–205.

(194) McGuire, B. A.; Loomis, R. A.; Burkhardt, A. M.; Lee, K. L. K.; Shingledecker, C. N.; Charnley, S. B.; Cooke, I. R.; Cordiner, M. A.; Herbst, E.; Kalenskii, S. et al. Detection of Two Interstellar Polycyclic Aromatic Hydrocarbons via Spectral Matched Filtering. *Science* **2021**, *371*, 1265.

(195) Burkhardt, A. M.; Lee, K. L. K.; Changala, P. B.; Shingledecker, C. N.; Cooke, I. R.; Loomis, R. A.; Wei, H.; Charnley, S. B.; Herbst, E.; McCarthy, M. C. et al. Discovery of the Pure Polycyclic Aromatic Hydrocarbon Indene (c-C_9H_8) with GOTHAM Observations of TMC-1. *Astrophys. J. Lett.* **2021**, *913*, L18.

(196) Cernicharo, J.,; Agúndez, M.,; Cabezas, C.,; Tercero, B.,; Marcelino, N.,; Pardo, J. R.,; de Vicente, P., Pure hydrocarbon cycles in TMC-1: Discovery of ethynyl cyclopropenylidene, cyclopentadiene, and indene. *A&A* **2021**, *649*, L15.

(197) Cernicharo, J.; Heras, A. M.; Tielens, A. G. G. M.; Pardo, J. R.; Herpin, F.; Guélin, M.; Waters, L. B. F. M. Infrared Space Observatory's Discovery of C_4H_2, C_6H_2, and Benzene in CRL 618. *Astrophys. J.* **2001**, *546*, L123–L126.

(198) Langhoff, S. R. Theoretical Infrared Spectra for Polycyclic Aromatic Hydrocarbon Neutrals, Cations, and Anions. *J. Phys. Chem.* **1996**, *100*, 2819–2841.

(199) Bauschlicher, Jr., C. W.; Ricca, A. The Infrared Spectra of Polycylic Aromatic Hydrocarbons with Some or All Hydrogen Atoms Removed. *Astrophys. J.* **2013**, *776*, 102.

(200) Boersma, C.; Bauschlicher, Jr., C. W.; Ricca, A.; Mattioda, A. L.; Cami, J.; Peeters, E.; de Armas, F. S.; Saborido, G. P.; Hudgins, D. M.; Allamandola, L. J. The NASA Ames PAH IR Spectroscopic Database Version 2.00: Updated Content, Web Site, and On(Off)line Tools. *Astrophys. J. Suppl. Ser.* **2014**, *211*, 8.

(201) Ricca, A.; Bauschlicher, Jr., C. W.; Boersma, C.; Tielens, A. G. G. M.; Allamandola, L. J. The Infrared Spectroscopy of Compact Polycyclic Aromatic Hydrocarbons Containing Up To 384 Carbons. *Astrophys. J.* **2012**, *754*, 75.

(202) Martin, J. M. L.; Taylor, P. R. Accurate *ab Initio* Quartic Force Field for *trans*-HNNH and Treatment of Resonance Polyads. *Spectrochim. Acta A* **1997**, *53*, 1039–1050.

(203) Mackie, C. J.; Candian, A.; Maltseva, E.; Petrignani, A.; Oomens, J.; Lee, W. J. B. T. J.; Tielens, A. G. G. M. The Anharmonic Quartic Force Field Infrared Spectra of Three Polycyclic Aromatic Hydrocarbons: Naphthalene, Anthracene, and Tetracene. *J. Chem. Phys.* **2015**, *143*, 224314.

(204) Maltseva, E.; Petrignani, A.; Candian, A.; Mackie, C. J.; Huang, X.; Lee, T. J.; Tielens, A. G. G. M.; Oomens, J.; Buma, W. J. High-Resolution IR Absorption Spectroscopy of Polycyclic Aromatic Hydrocarbons: The Realm of Anharmonicity. *Astrophys. J.* **2015**, *814*, 23.

(205) Hamprecht, F. A.; Cohen, A. J.; Tozer, D. J.; Handy, N. C. Development and Assessment of New Exchange-Correlation Functionals. *J. Chem. Phys.* **1998**, *109*, 6264–6271.

(206) Frisch, M. J.; Trucks, G. W.; Schlegel, H. B.; Scuseria, G. E.; Robb, M. A.; Cheeseman, J. R.; Scalmani, G.; Barone, V.; Petersson, G. A.; Nakatsuji, H. et al. Gaussian 16 Revision C.01. 2016; Gaussian Inc. Wallingford CT.

(207) Mackie, C. J.; Candian, A.; Huang, X.; Maltseva, E.; Petrignani, A.; Oomens, J.; Mattioda, A. L.; Buma, W. J.; Lee, T. J.; Tielens, A. G. G. M. The Anharmonic

Quartic Force Field Infrared Spectra of Five Non-Linear Polycyclic Aromatic Hydrocarbons: Benz[a]anthracene, Chrysene, Phenanthrene, Pyrene, and Triphenylene. *J. Chem. Phys.* **2016**, *145*, 084313.

(208) Mackie, C. J.; Candian, A.; Huang, X.; Maltseva, E.; Petrignani, A.; Oomens, J.; Buma, W. J.; Lee, T. J.; Tielens, A. G. G. M. The Anharmonic Quartic Force Field Infrared Spectra of Hydrogenated and Methylated PAHs. *Phys. Chem. Chem. Phys.* **2018**, *20*, 1189–1197.

(209) Becke, A. D. Density-Functional Thermochemistry. III. The Role of Exact Exchange. *J. Chem. Phys.* **1993**, *98*, 5648–5652.

(210) Yang, W. T.; Parr, R. G.; Lee, C. T. Various Functionals for the Kinetic Energy Density of an Atom or Molecule. *Phys. Rev. A* **1986**, *34*, 4586–4590.

(211) Lee, C.; Yang, W. T.; Parr, R. G. Development of the Colle-Salvetti Correlation-Energy Formula into a Functional of the Electron Density. *Phys. Rev. B.* **1988**, *37*, 785–789.

(212) Barone, V.; Cimino, P.; Stendardo, E. Development and Validation of the B3LYP/N07D Computational Model for Structural Parameter and Magnetic Tensors of Large Free Radicals. *J. Chem. Theory Comput.* **2008**, *4*, 751–764.

(213) Peeters, E.; Allamandola, L. J.; Hudgins, D. M.; Hony, S.; Tielens, A. G. G. M. In *Astrophysics of Dust, ASP Conference Series*; Witt, A. N., Clayton, G. C., Draine, B. T., Eds.; Astronomical Society of the Pacific: San Francisco, CA, 2004; Vol. 309.

(214) Peeters, E.; Mackie, C.; Candian, A.; Tielens, A. G. G. M. A Spectroscopic View on Cosmic PAH Emission. *Accounts of Chemical Research* **2021**, *54*, 1921–1933.

(215) Huang, X.; Schwenke, D. W.; Lee, T. J. What It Takes to Compute Highly Accurate

Rovibrational Line Lists for Use in Astrochemistry. *Acc. Chem. Res.* **2021**, *54*, 1311–1321.

(216) Tennyson, J.; Zobov, N. F.; Williamson, R.; Polyansky, O. L. Experimental Energy Levels of the Water Molecule. *J. Phys. Chem. Ref. Data* **2001**, *30*, 735.

(217) Rey, M.; Nikitin, A. V.; Babikov, Y. L.; Tyuterev, V. G. TheoReTS – An Information System for Theoretical Spectra Based on Variational Predictions from Molecular Potential Energy and Dipole Moment Surfaces. *J. Molec. Spectrosc.* **2016**, *327*, 138–158.

(218) Partridge, H.; Schwenke, D. W. The Determination of an Accurate Isotope Dependent Potential Energy Surface for Water from Extensive *ab Initio* Calculations and Experimental Data. *J. Chem. Phys.* **1997**, *106*, 4618–4639.

(219) Fortney, J. J.; Robinson, T. D.; Domagal-Goldman, S.; Genio, A. D. D.; Gordon, I. E.; Gharib-Nezhad, E.; Lewis, N.; Sousa-Silva, C.; Airapetian, V.; Drouin, B. et al. The Need for Laboratory Measurements and Ab Initio Studies to Aid Understanding of Exoplanetary Atmospheres. 2019; `http://arxiv.org/abs/1905.07064`.

(220) Huang, X.; Schwenke, D. W.; Tashkun, S. A.; Lee, T. J. An Isotopic-Independent Highly Accurate Potential Energy Surface for CO_2 Isotopologues and *ab Initio* $^{12}C^{16}O_2$ Infrared Line List. *J. Chem. Phys.* **2012**, *136*, 124311.

(221) Huang, X.; Freedman, R. S.; Tashkun, S. A.; Schwenke, D. W.; Lee, T. J. Semi-Empirical $^{12}C^{16}O_2$ IR Line Lists for Simulations up to 1500K and 20,000 cm^{-1}. *J. Quant. Spec. Rad. Trans.* **2013**, *130*, 134–146, HITRAN2012 special issue.

(222) Huang, X.; Gamache, R. R.; Freedman, R. S.; Schwenke, D. W.; Lee, T. J. Reliable Infrared Line Lists for 13 CO_2 Isotopologues up to E'= 18,000 cm^{-1} and 1500 K, with Line Shape Parameters. *J. Quant. Spec. Rad. Trans.* **2014**, *147*, 134–144.

(223) Huang, X.; Schwenke, D. W.; Freedman, R. S.; Lee, T. J. Ames-2016 Line Lists for 13 Isotopologues of CO_2: Updates, Consistency, and Remaining Issues. *J. Quant. Spec. Rad. Trans.* **2017**, *203*, 224–241, HITRAN2016 Special Issue.

(224) Huang, X.; Schwenke, D. W.; Lee, T. J. Isotopologue Consistency of Semi-Empirically Computed Infrared Line Lists and Further Improvement for Rare Isotopologues: CO_2 and SO_2 Case Studies. *J. Quant. Spec. Rad. Trans.* **2019**, *230*, 222–246.

(225) Gamache, R. R.; Roller, C.; Lopes, E.; Gordon, I. E.; Rothman, L. S.; Polyansky, O. L.; Zobov, N. F.; Kyuberis, A. A.; Tennyson, J.; Yurchenko, S. N. et al. Total Internal Partition Sums for 166 Isotopologues of 51 Molecules Important in Planetary Atmospheres: Application to HITRAN2016 and Beyond. *J. Quant. Spec. Rad. Trans.* **2017**, *203*, 70–87, HITRAN2016 Special Issue.

(226) Tarczay, G.; Császár, A. G.; Klopper, W.; Szalay, V.; Allen, W. D.; Schaefer, III, H. F. The Barrier to Linearity of Water. *J. Chem. Phys.* **1999**, *110*, 11971–11981.

(227) Polyansky, O. L.; Zobov, N. F.; Mizus, I. I.; Lodi, L.; Yurchenko, S. N.; Tennyson, J.; Császár, A. G.; Boyarkin, O. V. Global Spectroscopy of the Water Monomer. *Phil. Trans. Royal Soc. A* **2012**, *370*, 2728–2748.

(228) Cheung, A. C.; Rank, D. M.; Townes, C. H.; Thornton, D. D.; Welch, W. J. Detection of NH_3 Molecules in the Interstellar Medium by Their Microwave Emission. *Phys. Rev. Lett.* **1968**, *21*, 1701–1705.

(229) V. N. Salinas, M. R. H.; Bergin, E. A.; Cleeves, L. I.; Brinch, C.; Blake, G. A.; Lis, D. C.; Melnick, G. J.; Panić, O.; Pearson, J. C.; Kristensen, L. et al. First Detection of Gas-Phase Ammonia in a Planet-Forming Disk. NH_3, N_2H^+, and H_2O in the Disk around TW Hydrae. *Astron. Astrophys.* **2016**, *591*, 122.

(230) Fink, U.; Larson, H. P.; Bjoraker, G. L.; Johnson, J. R. The NH_3 Spectrum in Saturn's 5 Micron Window. *Astrophys. J.* **1983**, *268*, 880–888.

(231) Huang, X.; Schwenke, D. W.; Lee, T. J. Rovibrational Spectra of Ammonia. I. Unprecedented Accuracy of a Potential Energy Surface Used with Nonadiabatic Corrections. *J. Chem. Phys.* **2011**, *134*, 044320.

(232) Huang, X.; Schwenke, D. W.; Lee, T. J. An Accurate Global Potential Energy Surface, Dipole Moment Surface, and Rovibrational Frequencies for NH_3. *J. Chem. Phys.* **2008**, *129*, 214304.

(233) Müller, H. S.; Schlöder, F.; Stutzki, J.; Winnewisser, G. The Cologne Database for Molecular Spectroscopy, CDMS: a useful tool for astronomers and spectroscopists. *J. Molec. Struct.* **2005**, *742*, 215–227.

(234) Huang, X.; Schwenke, D. W.; Lee, T. J. Rovibrational Spectra of Ammonia. II. Detailed Analysis, Comparison, and Prediction of Spectroscopic Assignments for $^{14}NH_3$, $^{15}NH_3$, and $^{14}ND_3$. *J. Chem. Phys.* **2011**, *134*, 044321.

(235) Sung, K.; Brown, L. R.; Huang, X.; Schwenke, D. W.; Lee, T. J.; Coy, S. L.; Lehmann, K. K. Extended Line Positions, Intensities, Empirical Lower State Energies and Quantum Assignments of NH_3 from 6300 to 7000 cm^{-1}. *J. Quant. Spec. Rad. Trans.* **2012**, *113*, 1066–1083, Three Leaders in Spectroscopy.

(236) Huang, X.; Schwenke, D. W.; Lee, T. J. Ames $^{32}S^{16}O^{18}O$ Line List for High-Resolution Experimental IR Analysis. *J. Molec. Spectrosc.* **2016**, *330*, 101–111.

(237) Stewart, A. I.; Anderson, D. E.; Esposito, L. W.; Barth, C. A. Ultraviolet Spectroscopy of Venus: Initial Results from the Pioneer Venus Orbiter. *Science* **1979**, *203*, 777–779.

(238) Hintze, P. E.; Kjaergaard, H. G.; Vaida, V.; Burkholder, J. B. Vibrational and Electronic Spectroscopy of Sulfuric Acid Vapor. *J. Phys. Chem. A* **2003**, *107*, 1112–1118.

(239) Snyder, L. E.; Hollis, J. M.; Ulich, B. L.; Lovas, F. J.; Johnson, D. R.; Buhl, D. Radio Detection of Interstellar Sulfur Dioxide. *Astrophys. J.* **1975**, *198*, L81–L84.

(240) Huang, X.; Schwenke, D. W.; Lee, T. J. Empirical Infrared Line Lists for Five SO_2 Isotopologues: $^{32/33/34/36}S^{16}O_2$ and $^{32}S^{18}O_2$. *J. Molec. Spectrosc.* **2015**, *311*, 19–24, Theory and Spectroscopy.

(241) Underwood, D. S.; Tennyson, J.; Yurchenko, S. N.; Huang, X.; Schwenke, D. W.; Lee, T. J.; Clausen, S.; Fateev, A. ExoMol Molecular Line Lists – XIV. The Rotation–Vibration Spectrum of Hot SO_2. *Monthly Notices of the Royal Astronomical Society* **2016**, *459*, 3890–3899.

(242) Huang, X.; Schwenke, D. W.; Lee, T. J. Exploring the Limits of the Data-Model-Theory Synergy: "Hot" MW Transitions for Rovibrational IR Studies. *J. Molec. Spectrosc.* **2020**, *1217*, 128260.

(243) Sousa-Silva, C.; Seager, S.; Ranjan, S.; Petkowski, J. J.; Zhan, Z.; Hu, R.; Bains, W. Phosphine as a Biosignature Gas in Exoplanet Atmospheres. *Astrobiology* **2020**, *20*, 235–268.

(244) Tielens, A. G. G. M. *Molecular Astrophysics*; Cambridge University Press: Cambridge, UK, 2021.

(245) Allamandola, L. J.; Tielens, A. G. G. M.; Baker, J. R. Interstellar Polycyclic Aromatic Hydrocarbons: The Infrared Emission Bands, the Excitation/Emission Mechanism, and the Astrophysical Implications. *Astrophys. J. Suppl. Ser.* **1989**, *71*, 733–775.

(246) Puget, J. L.; Leger, A. A New Component of the Interstellar Matter: Small Grains and Large Aromatic Molecules. *Annual Rev. Astron. Astrophys.* **1989**, *27*, 161–198.

(247) Mackie, C. J.; Chen, T.; Candian, A.; Lee, T. J.; Tielens, A. G. G. M. Fully Anharmonic Infrared Cascade Spectra of Polycyclic Aromatic Hydrocarbons. *J. Chem. Phys.* **2018**, *149*, 134302.

(248) Bauschlicher, Jr., C. W.; Boersma, C.; Ricca, A.; Mattioda, A. L.; Cami, J.; Peeters, E.; Sánchez de Armas, F.; Puerta Sabroido, G.; Hudgins, D. M.; Allamandola, L. J. The NASA Ames Polycyclic Aromatic Hydrocarbon Infrared Spectroscopic Database: The Computed Spectra. *Astrophys. J. Suppl. Ser.* **2010**, *189*, 341–351.

(249) Bauschlicher, Jr., C. W.; Ricca, A.; Boersma, C.; Allamandola, L. J. The NASA Ames PAH IR Spectroscopic Database: Computational Version 3.00 with Updated Content and the Introduction of Multiple Scaling Factors. *Astrophys. J. Suppl. Ser.* **2018**, *234*, 32.

(250) Mattioda, A. L.; Hudgins, D. M.; Boersma, C.; Bauschlicher, Jr., C. W.; Ricca, A.; Cami, J.; Peeters, E.; Sánchez de Armas, F.; Puerta Saborido, G.; Allamandola, L. J. The NASA Ames PAH IR Spectroscopic Database: The Laboratory Spectra. *Astrophys. J. Suppl. Ser.* **2020**, *251*, 22.

(251) Hoy, A. R.; Mills, I. M.; Strey, G. Anharmonic Force Constant Calculations. *Mol. Phys.* **1972**, *24*, 1265–1290.

(252) Califano, S. *Vibrational States*; Wiley: London, 1976.

(253) Boersma, C.; Bauschlicher, Jr., C. W.; Ricca, A.; Mattioda, A. L.; Peeters, E.; Tielens, A. G. G. M.; Allamandola, L. J. Polycyclic Aromatic Hydrocarbon Far-infrared Spectroscopy. *Astrophys. J.* **2011**, *729*, 64.

(254) Tielens, A. G. G. M. Interstellar Polycyclic Aromatic Hydrocarbon Molecules. *Annu. Rev. Astron. Astrophys.* **2008**, *46*, 289–337.

(255) Maragkoudakis, A.; Peeters, E.; Ricca, A. Probing the Size and Charge of Polycyclic Aromatic Hydrocarbons. *Mon. Not. Royal Astron. Soc.* **2020**, *494*, 642–664.

(256) Maltseva, E.; Petrignani, A.; Candian, A.; Mackie, C. J.; Huang, X.; Lee, T. J.; Tielens, A. G. G. M.; Oomens, J.; Buma, W. J. High-Resolution IR Absorption Spec-

troscopy of Polycyclic Aromatic Hydrocarbons in the 3 μm Region: Role of Hydrogenation and Alkylation. *Astrophys. J.* **2016**, *831*, 58.

(257) Maltseva, E.; Mackie, C. J.; Candian, A.; Petrignani, A.; Huang, X.; Lee, T. J.; Tielens, A. G. G. M.; Oomens, J.; Buma, W. J. High-Resolution IR Absorption Spectroscopy of Polycyclic Aromatic Hydrocarbons in the 3 μm Region: Role of Periphery. *Astron. Astrophys.* **2018**, *610*, A65.

(258) Boese, A. D.; Martin, J. M. L. Vibrational Spectra of the Azabenzenes Revisited: Anharmonic Force Fields. *J. Phys. Chem. A* **2004**, *108*, 3085–3096.

(259) Barone, V.; Cimino, P.; Stendardo, E. Development and Validation of the B3LYP/N07D Computational Model for Structural Parameter and Magnetic Tensors of Large Free Radicals. *J. Chem. Theory Comput.* **2008**, *4*, 751–764.

(260) Martin, J. M. L.; Lee, T. J.; Taylor, P. R.; François, J.-P. The Anharmonic Force Field of Ethylene, C_2H_4, by Means of Accurate *ab Initio* Calculations. *J. Chem. Phys.* **1995**, *103*, 2589–2602.

(261) Basire, M.; Parneix, P.; Calvo, F.; Pino, T.; Bréchignac, P. Temperature and Anharmonic Effects on the Infrared Absorption Spectrum from a Quantum Statistical Approach: Application to Naphthalene. *J. Phys. Chem. A* **2009**, *113*, 6947–6954.

(262) Basire, M.; Parneix, P.; Calvo, F. Quantum Anharmonic Densities of States Using the Wang–Landau Method. *J. Chem. Phys.* **2011**, *129*, 081101.

(263) Calvo, F.; Basire, M.; Parneix, P. Temperature Effects on the Rovibrational Spectra of Pyrene-Based PAHs. *J. Phys. Chem. A* **2011**, *115*, 8845–8854.

(264) Chen, T.; Mackie, C. J.; Candian, A.; Lee, T. J.; Tielens, A. G. G. M. Anharmonicity and the IR Emission Spectrum of Highly Excited PAHs. *Astron. Astrophys.* **2018**, *618*, A49.

(265) Wagner, D.; Kim, H.; Saykally, R. Peripherally Hydrogenated Neutral Polycyclic Aromatic Hydrocarbons as Carriers of the 3 Micron Interstellar Infrared Emission Complex: Results from Single-Photon Infrared Emission Spectroscopy. *Astrophys. J.* **2000**, *545*, 854–860.

(266) Mackie, C. J.; Candian, A.; Lee, T. J.; Tielens, A. G. G. M. Modelling the Infrared Cascade Spectra of Anharmonic Interstellar PAHs: the 11.2 μm Band. *Theo. Chem. Acc.* **2021**, *140*, 124.